

Heavy ion event generator HYDJET++ (HYDroynamics plus JETs)

I.P. Lokhtin¹, L.V. Malinina, S.V. Petrushanko, A.M. Snigirev

*M.V. Lomonosov Moscow State University, D.V. Skobeltsyn Institute of Nuclear
Physics, Moscow, Russia*

I. Arsene², K. Tywoniuk³

The Department of Physics, University of Oslo, Norway

Abstract

HYDJET++ is a Monte-Carlo event generator for simulation of relativistic heavy ion AA collisions considered as a superposition of the soft, hydro-type state and the hard state resulting from multi-parton fragmentation. This model is the development and continuation of HYDJET event generator (Lokhtin & Snigirev, 2006, EPJC, 45, 211). The main program is written in the object-oriented C++ language under the ROOT environment. The hard part of HYDJET++ is identical to the hard part of Fortran-written HYDJET and it is included in the generator structure as a separate directory. The soft part of HYDJET++ event is the “thermal” hadronic state generated on the chemical and thermal freeze-out hypersurfaces obtained from the parameterization of relativistic hydrodynamics with preset freeze-out conditions. It includes the longitudinal, radial and elliptic flow effects and the decays of hadronic resonances. The corresponding fast Monte-Carlo simulation procedure, C++ code FAST MC (Amelin et al., 2006, PRC, 74, 064901; 2008, PRC, 77, 014903) is adapted to HYDJET++. It is designed for studying the multi-particle production in a wide energy range of heavy ion experimental facilities: from FAIR and NICA to RHIC and LHC.

PACS: 24.10.Lx, 24.85.+p, 25.75.-q, 25.75.Bh, 25.75.Dw, 25.75.Ld, 25.75.Nq

Key words: Monte-Carlo event generators, relativistic heavy ion collisions, hydrodynamics, QCD jets, partonic energy loss, flow, quark-gluon plasma

¹ Corresponding author

² On leave from the Institute for Space Sciences, Bucharest, Romania

³ Current affiliation: Departamento de Física de Partículas, Universidad de Santiago de Compostela, Santiago de Compostela, Espana

PROGRAM SUMMARY

Manuscript Title: Heavy ion event generator HYDJET++ (HYDroynamics plus JETs)

Authors: Igor Lokhtin, Ludmila Malinina, Sergey Petrushanko, Alexander Snigirev, Ionut Arsene, Konrad Tywoniuk

Program Title: HYDJET++, version 2.0

Programming language: C++ (however there is a Fortran-written part which is included in the generator structure as a separate directory)

Size of the package: 3.5 MBytes directory and 800 kBytes compressed distribution archive (without ROOT libraries). The output file created by the code in ROOT tree format for 100 central (0–5%) Au+Au events at $\sqrt{s} = 200A$ GeV (Pb+Pb events at $\sqrt{s} = 5500A$ GeV) with default input parameters requires 40 (190) MBytes of the disk space.

Computer: PC - hardware independent (both C++ and Fortran compilers and ROOT environment [1] should be installed)

Operating system: Linux (Scientific Linux, Red Hat Enterprise, FEDORA, etc.)

RAM: 50 MBytes (determined by ROOT requirements)

Number of processors used: 1

Keywords: Monte-Carlo event generators, relativistic heavy ion collisions, hydrodynamics, QCD jets, partonic energy loss, flow, quark-gluon plasma

PACS: 24.10.Lx, 24.85.+p, 25.75.-q, 25.75.Bh, 25.75.Dw, 25.75.Ld, 25.75.Nq

Classification: 11.2 Elementary particle physics, phase space and event simulation

External routines/libraries: ROOT (any version)

Subprograms used: PYTHIA event generator (version 6.401 or later), PYQUEN event generator (version 1.5 or later)

Nature of the physical problem:

The experimental and phenomenological study of multi-particle production in relativistic heavy ion collisions is expected to provide valuable information on the dynamical behaviour of strongly-interacting matter in the form of quark-gluon plasma (QGP) [2–4], as predicted by lattice Quantum Chromodynamics (QCD) calculations. Ongoing and future experimental studies in a wide range of heavy ion beam energies require the development of new Monte-Carlo (MC) event generators and improvement of existing ones. Especially for experiments at the CERN Large Hadron Collider (LHC), implying very high parton and hadron multiplicities, one needs

fast (but realistic) MC tools for heavy ion event simulations [5–7]. The main advantage of MC technique for the simulation of high-multiplicity hadroproduction is that it allows a visual comparison of theory and data, including if necessary the detailed detector acceptances, responses and resolutions. The realistic MC event generator has to include maximum possible number of observable physical effects, which are important to determine the event topology: from the bulk properties of soft hadroproduction (domain of low transverse momenta $p_T \lesssim 1\text{GeV}/c$) such as collective flows, to hard multi-parton production in hot and dense QCD-matter, which reveals itself in the spectra of high- p_T particles and hadronic jets. Moreover, the role of hard and semi-hard particle production at LHC can be significant even for the bulk properties of created matter, and hard probes of QGP became clearly observable in various new channels [8–11]. In majority of the available MC heavy ion event generators, the simultaneous treatment of collective flow effects for soft hadroproduction and hard multi-parton in-medium production (medium-induced partonic rescattering and energy loss, so called “jet quenching”) is lacking. Thus, in order to analyze existing data on low and high- p_T hadron production, test the sensitivity of physical observables at the upcoming LHC experiments (and other future heavy ion facilities) to the QGP formation, and study the experimental capabilities of constructed detectors, the development of adequate and fast MC models for simultaneous collective flow and jet quenching simulations is necessary. HYDJET++ event generator includes detailed treatment of soft hadroproduction as well as hard multi-parton production, and takes into account known medium effects.

Solution method:

A heavy ion event in HYDJET++ is a superposition of the soft, hydro-type state and the hard state resulting from multi-parton fragmentation. Both states are treated independently. HYDJET++ is the development and continuation of HYDJET MC model [12]. The main program is written in the object-oriented C++ language under the ROOT environment [1]. The hard part of HYDJET++ is identical to the hard part of Fortran-written HYDJET [13] (version 1.5) and is included in the generator structure as a separate directory. The routine for generation of single hard NN collision, generator PYQUEN [12,14], modifies the “standard” jet event obtained with the generator PYTHIA_6.4 [15]. The event-by-event simulation procedure in PYQUEN includes 1) generation of initial parton spectra with PYTHIA and production vertexes at given impact parameter; 2) rescattering-by-rescattering simulation of the parton path in a dense zone and its radiative and collisional energy loss; 3) final hadronization according to the Lund string model for hard partons and in-medium emitted gluons. Then the PYQUEN multi-jets generated according to the binomial distribution are included in the hard part of the event. The mean number of jets produced in an AA event is the product of the number of binary NN sub-collisions at a given impact parameter and the integral cross section of the hard process in NN collisions with the minimum transverse momentum transfer p_T^{\min} . In order to take into account the effect of nuclear shadowing on parton distribution functions, the impact parameter dependent parameterization obtained in the framework of Glauber-Gribov theory [16] is used. The soft part of HYDJET++ event is the “thermal” hadronic state generated on the chemical and thermal freeze-out hy-

persurfaces obtained from the parameterization of relativistic hydrodynamics with preset freeze-out conditions (the adapted C++ code FAST MC [17,18]). Hadron multiplicities are calculated using the effective thermal volume approximation and Poisson multiplicity distribution around its mean value, which is supposed to be proportional to the number of participating nucleons at a given impact parameter of AA collision. The fast soft hadron simulation procedure includes 1) generation of the 4-momentum of a hadron in the rest frame of a liquid element in accordance with the equilibrium distribution function; 2) generation of the spatial position of a liquid element and its local 4-velocity in accordance with phase space and the character of motion of the fluid; 3) the standard von Neumann rejection/acceptance procedure to account for the difference between the true and generated probabilities; 4) boost of the hadron 4-momentum in the center mass frame of the event; 5) the two- and three-body decays of resonances with branching ratios taken from the SHARE particle decay table [19]. The high generation speed in HYDJET++ is achieved due to almost 100% generation efficiency of the “soft” part because of the nearly uniform residual invariant weights which appear in the freeze-out momentum and coordinate simulation. Although HYDJET++ is optimized for very high energies of RHIC and LHC colliders (c.m.s. energies of heavy ion beams $\sqrt{s} = 200$ and 5500 GeV per nucleon pair respectively), in practice it can also be used for studying the particle production in a wider energy range down to $\sqrt{s} \sim 10$ GeV per nucleon pair at other heavy ion experimental facilities. As one moves from very high to moderately high energies, the contribution of the hard part of the event becomes smaller, while the soft part turns into just a multi-parameter fit to the data.

Restrictions:

HYDJET++ is only applicable for symmetric AA collisions of heavy ($A \gtrsim 40$) ions at high energies (c.m.s. energy $\sqrt{s} \gtrsim 10$ GeV per nucleon pair). The results obtained for very peripheral collisions (with the impact parameter of the order of two nucleus radii, $b \sim 2R_A$) and very forward rapidities may be not adequate.

Running time:

The generation of 100 central (0–5%) Au+Au events at $\sqrt{s} = 200A$ GeV (Pb+Pb events at $\sqrt{s} = 5500A$ GeV) with default input parameters takes about 7 (85) minutes on a PC 64 bit Intel Core Duo CPU @ 3 GHz with 8 GB of RAM memory under Red Hat Enterprise.

Accessibility:

<http://cern.ch/lokhtin/hydjet++>

References for the physics model:

- [1] I.P. Lokhtin, A.M. Snigirev, Eur. Phys. J. C 46 (2006) 211.
- [2] N.S. Amelin, R. Lednicky, T.A. Pocheptsov, I.P. Lokhtin, L.V. Malinina, A.M. Snigirev, Iu.A. Karpenko and Yu.M. Sinyukov, Phys. Rev. C 74 (2006) 064901.
- [3] N.S. Amelin, I. Arsene, L. Bravina, Iu.A. Karpenko, R. Lednicky, I.P. Lokhtin, L.V. Malinina, A.M. Snigirev and Yu.M. Sinyukov, Phys. Rev. C 77 (2008) 014903.

1 Introduction

One of the basic tasks of modern high energy physics is the study of the fundamental theory of strong interaction (Quantum Chromodynamics, QCD) in new, unexplored extreme regimes of super-high densities and temperatures through the investigation of the properties of hot and dense multi-parton and multi-hadron systems produced in high-energy nuclear collisions [20–22]. Indeed, QCD is not just a quantum field theory with an extremely rich dynamical content (such as asymptotic freedom, chiral symmetry, non-trivial vacuum topology, strong CP violation problem, colour superconductivity), but perhaps the only sector of the Standard Model, where the basic features (as phase diagram, phase transitions, thermalisation of fundamental fields) may be the subject to scrutiny in the laboratory. The experimental and phenomenological study of multi-particle production in ultrarelativistic heavy ion collisions [2–4] is expected to provide valuable information on the dynamical behaviour of QCD matter in the form of a quark-gluon plasma (QGP), as predicted by lattice calculations.

Experimental data, obtained from the Relativistic Heavy Ion Collider (RHIC) at maximum beam energy in the center of mass system of colliding ions $\sqrt{s} = 200$ GeV per nucleon pair, supports the picture of formation of a strongly interacting hot QCD matter (“quark-gluon fluid”) in the most central Au+Au (and likely Cu+Cu) collisions [23–26]. This appears as significant modification of properties of multi-particle production in heavy ion collisions as compared with the corresponding proton-proton (or peripheral heavy ion) interactions. In particular, one of the important perturbative (“hard”) probes of QGP is the medium-induced energy loss of energetic partons, so called “jet quenching” [27], which is predicted to be very different in cold nuclear matter and in QGP, and leads to a number of phenomena which are already seen in the RHIC data on the qualitative level, such as suppression of high- p_T hadron production, modification of azimuthal back-to-back correlations, azimuthal anisotropy of hadron spectra at high p_T , etc. [28]. On the other hand, one of the most spectacular features of low transverse momentum (“soft”) hadroproduction at RHIC are strong collective flow effects: the radial flow (ordering of the mean transverse momentum of hadron species with corresponding mass) and the elliptic flow (mass-ordered azimuthal anisotropy of particle yields with respect to the reaction plane in non-central collisions). The development of such a strong flow is well described by the hydrodynamic models and requires short time scale and large pressure gradients, attributed to strongly interacting systems [29]. Note however, that results of hydrodynamic models usually disagree with the data on femtoscopic momentum correlations, resulting from the space-time characteristics of the system at freeze-out stage.

The heavy ion collision energy in Large Hadron Collider (LHC) at CERN

a factor of 30 larger than that in RHIC, thereby allows one to probe new frontiers of super-high temperature and (almost) net-baryon free QCD [8–11]. The emphasis of the LHC heavy ion data analysis (at $\sqrt{s} = 5.5$ TeV per nucleon pair for lead beams) will be on the perturbative, or hard probes of the QGP (quarkonia, jets, photons, high- p_T hadrons) as well as on the global event properties, or soft probes (collective radial and elliptic flow effects, hadron multiplicity, transverse energy densities and femtoscopic momentum correlations). It is expected that at LHC energies the role of hard and semi-hard particle production will be significant even for the bulk properties of created matter.

Another domain of QCD phase diagram is high baryon density region, which can be probed in the future experimental studies at relatively moderate heavy ion beam energies $\sqrt{s} \sim 10$ GeV per nucleon pair (projects CBM [30] and MPD [31] at accelerator facilities FAIR-GSI and NICA-JINR, programs for heavy ion runs with lower beam energies at SPS and RHIC). These studies are motivated by the intention to search for the “critical point” of the quark-hadron phase transition, predicted by lattice QCD, where the type of transition is changing from smooth “crossover” (at high temperatures and low net-baryon densities) to first order transition (at high net-baryon densities and low temperatures) [32].

Ongoing and future experimental studies of relativistic heavy ion collisions in a wide range of beam energies require the development of new Monte-Carlo (MC) event generators and improvement of existing ones. Especially for experiments which will be conducted at LHC, due to very high parton and hadron multiplicities, one needs fast (but realistic) MC tools for heavy ion event simulation [5–7]. The main advantage of MC technique for the simulation of high-multiplicity hadroproduction is that it allows a visual comparison of theory and data, including if necessary the detailed detector acceptances, responses and resolutions. A realistic MC event generator should include a maximum possible number of observable physical effects which are important to determine the event topology: from the bulk properties of soft hadroproduction (domain of low transverse momenta $p_T \lesssim 1\text{GeV}/c$) such as collective flows, to hard multi-parton production in hot and dense QCD-matter, which reveals itself in the spectra of high- p_T particles and hadronic jets.

In most of the available MC heavy ion event generators, the simultaneous treatment of collective flow effects for soft hadroproduction and hard multi-parton in-medium production is absent. For example, the popular MC model HIJING [33] includes jet production and jet quenching on some level, but it does not include any significant flow effects. The recently developed MC model JEWEL [34], which combines a perturbative final state parton shower with QCD-medium effects, is actually not a heavy ion event generator, but rather a simulator of jet quenching in individual nucleon-nucleon sub-collisions

(like PYQUEN [12,14]). The event generators FRITIOF [35] and LUCIAE [36] include jet production (but without jet quenching), while some collective nuclear effects (such as string interactions and hadron rescatterings) are taken into account in LUCIAE. Another MC model THERMINATOR [37] includes detailed statistical description of “thermal” soft particle production and can reproduce the main bulk features of hadron spectra at RHIC (in particular, describe simultaneously the momentum-space measurements and the freeze-out coordinate-space data), but it does not include hard parton production processes. There is a number of microscopic transport hadron models (UrQMD [38], QGSM [39], AMPT [40], etc.), which attempt to analyze the soft particle production in a wide energy range, however they also do not include in-medium production of high- p_T multi-parton states. Moreover, hadronic cascade models have difficulties with the detailed description of relatively low- p_T RHIC data on elliptic flow and the size of hadron emission, obtained from momentum correlation measurements (e.g. AMPT can reproduce the elliptic flow or the correlation radii using different sets of model parameters). Another heavy ion event generator, ZPC [41], has been created to simulate parton cascade evolution in ultrarelativistic heavy ion collisions. From a physical point of view, such an approach seems reasonable only for very high beam energies (RHIC, LHC). Note also that the full treatment of parton cascades requires enormous amount of CPU run time (especially for LHC).

Thus, in order to analyze existing data on low and high- p_T hadron production, test the sensitivity of physical observables at the upcoming LHC experiments (and other future heavy ion facilities) to the QCD-matter formation, and study the experimental capabilities of constructed detectors, the development of adequate and fast MC models for simultaneous collective flow and jet quenching simulation is necessary. HYDJET++ event generator includes detailed treatment of soft hadroproduction as well as hard multi-parton production, and takes into account medium-induced parton rescattering and energy loss. Although the model is optimized for very high energies of colliding nuclei (RHIC, LHC), in practice it can also be used for studying the multi-particle production at lower energies at other heavy ion experimental facilities as FAIR and NICA. Moving from very high to moderately high energies, the contribution of the hard part of the event becomes smaller, while the soft part turns into just a multi-parameter fit to the data. The heavy ion event in HYDJET++ is the superposition of two independent parts: the soft, hydro-type state and the hard state resulting from multi-parton fragmentation. Note that a conceptually similar approximation has been developed in [42] but, to our best knowledge, it is not implemented as an MC event generator.

The main program of HYDJET++ is written in the object-oriented C++ language under the ROOT environment [1]. The hard part of HYDJET++ is identical to the hard part of Fortran-written HYDJET (version 1.5) and it is included in the generator structure as a separate directory. The soft part of

HYDJET++ event is the “thermal” hadronic state generated on the chemical and thermal freeze-out hypersurfaces obtained from a parameterization of relativistic hydrodynamics with preset freeze-out conditions. It includes the longitudinal, radial and elliptic flow effects and the decays of hadronic resonances. The corresponding fast MC simulation procedure based on C++ code, FAST MC [17,18], was adapted to HYDJET++. The high generation speed in FAST MC is achieved due to almost 100% generation efficiency because of nearly uniform residual invariant weights which appear in the freeze-out momentum and coordinate simulation.

Let us indicate some physical restrictions of the model. HYDJET++ is only applicable for symmetric AA collisions of heavy ($A \gtrsim 40$) ions at high energies ($\sqrt{s} \gtrsim 10$ GeV). Since the hydro-type approximation for heavy ion collisions is considered to be valid for central and semi-central collisions, the results obtained for very peripheral collisions (with impact parameter of the order of two nucleus radii, $b \sim 2R_A$) may be not adequate. Nor do we expect a correct event description in the region of very forward rapidities, where the other mechanisms of particle production, apart from hydro-flow and jets, may be important.

2 Physics model

A heavy ion event in HYDJET++ is a superposition of the soft, hydro-type state and the hard state resulting from multi-parton fragmentation. Both states are treated independently.

2.1 Model for the hard multi-jet production

The model for the hard multi-parton part of HYDJET++ event is the same as that for HYDJET event generator. A detailed description of the physics framework of this model can be found in the corresponding paper [12]. The approach to the description of multiple scattering of hard partons in the dense QCD-matter (such as quark-gluon plasma) is based on the accumulative energy loss via the gluon radiation being associated with each parton scattering in the expanding quark-gluon fluid and includes the interference effect (QCD analog [43–47] of the well known Landau-Pomeranchuk-Migdal (LPM) effect in QED [48,49] for the emission of gluons with a finite formation time) using the modified radiation spectrum dE/dl as a function of decreasing temperature T . The basic kinetic integral equation for the energy loss ΔE as a function of initial energy E and path length L has the form

$$\Delta E(L, E) = \int_0^L dl \frac{dP(l)}{dl} \lambda(l) \frac{dE(l, E)}{dl}, \quad \frac{dP(l)}{dl} = \frac{1}{\lambda(l)} \exp(-l/\lambda(l)), \quad (1)$$

where l is the current transverse coordinate of a parton, dP/dl is the scattering probability density, dE/dl is the energy loss per unit length, $\lambda = 1/(\sigma\rho)$ is the in-medium mean free path, $\rho \propto T^3$ is the medium density at the temperature T , σ is the integral cross section for the parton interaction in the medium. Both collisional and radiative energy loss are taken into account in the model.

The partonic collisional energy loss due to elastic scatterings is treated in high-momentum transfer limit [50–52]:

$$\frac{dE^{col}}{dl} = \frac{1}{4T\lambda\sigma} \int_{\mu_D^2}^{t_{\max}} dt \frac{d\sigma}{dt} t, \quad (2)$$

where the dominant contribution to the differential scattering cross section is

$$\frac{d\sigma}{dt} \cong C \frac{2\pi\alpha_s^2(t)}{t^2} \frac{E^2}{E^2 - m_p^2}, \quad \alpha_s = \frac{12\pi}{(33 - 2N_f) \ln(t/\Lambda_{QCD}^2)} \quad (3)$$

for the scattering of a hard parton with energy E and mass m_p off the “thermal” parton with energy (or effective mass) $m_0 \sim 3T \ll E$. Here $C = 9/4, 1, 4/9$ for gg, gq and qq scatterings respectively, α_s is the QCD running coupling constant for N_f active quark flavors, and Λ_{QCD} is the QCD scale parameter which is of the order of the critical temperature of quark-hadron phase transition, $\Lambda_{QCD} \simeq T_c \simeq 200$ MeV. The integrated cross section σ is regularized by the Debye screening mass squared $\mu_D^2(T) \simeq 4\pi\alpha_s T^2(1 + N_f/6)$. The maximum momentum transfer $t_{\max} = [s - (m_p + m_0)^2][s - (m_p - m_0)^2]/s$ where $s = 2m_0E + m_0^2 + m_p^2$. The model simplification is that the collisional energy loss due to scatterings with low momentum transfer (resulting mainly from the interactions with plasma collective modes or colour background fields, see for recent developments [53–61] and references therein) is not considered here. Note, however, that in the majority of estimations, the latter process does not contribute much to the total collisional loss in comparison with the high-momentum scattering (due to absence of the large factor $\sim \ln(E/\mu_D)$), and in numerical computations it can be effectively “absorbed” by means of redefinition of minimum momentum transfer $t_{\min} \sim \mu_D^2$ in (2). Another model assumption is that the collisional loss represents the incoherent sum over all scatterings, although it was argued recently in [62] that interference effects may appear in elastic parton energy loss in a medium of finite size.

The partonic radiative energy loss is treated in the frameworks of BDMS formalism [63,64]. In fact, there are several calculations of the inclusive en-

ergy distribution of medium-induced gluon radiation using Feynman multiple scattering diagrams. The detailed discussions on the relation between these approaches, their basic parameters and physics predictions can be found in the recent proceedings of CERN TH Workshops (see [8,9] and references therein). In the BDMS approach, the strength of multiple scattering is characterized by the transport coefficient $\hat{q} = \mu_D^2/\lambda_g$ (λ_g is the gluon mean free path), which is related to the elastic scattering cross section σ in (3). In our simulations this strength is regulated mainly by the initial QGP temperature T_0 . Then the energy spectrum of coherent medium-induced gluon radiation and the corresponding dominant part of radiative energy loss of massless parton become [63,64]:

$$\frac{dE^{rad}}{dl} = \frac{2\alpha_s(\mu_D^2)C_R}{\pi L} \int_{\omega_{min}}^E d\omega \left[1 - y + \frac{y^2}{2} \right] \ln |\cos(\omega_1 \tau_1)|, \quad (4)$$

$$\omega_1 = \sqrt{i \left(1 - y + \frac{C_R}{3} y^2 \right) \bar{\kappa} \ln \frac{16}{\bar{\kappa}}} \quad \text{with} \quad \bar{\kappa} = \frac{\mu_D^2 \lambda_g}{\omega(1-y)}, \quad (5)$$

where $\tau_1 = L/(2\lambda_g)$, $y = \omega/E$ is the fraction of the hard parton energy carried away by the radiated gluon, and $C_R = 4/3$ is the quark color factor. A similar expression for the gluon jet can be obtained by setting $C_R = 3$ and properly changing the factor in the square brackets in (4) [63]. The integration (4) is carried out over all energies from $\omega_{min} = E_{LPM} = \mu_D^2 \lambda_g$, the minimum radiated gluon energy in the coherent LPM regime, up to initial parton energy E . Note that we do not consider here possible effects of double parton scattering [65,66] and thermal gluon absorption [67], which can be included in the model in the future.

The simplest generalization of the formula (4) for a heavy quark of mass m_q can be done by using the “dead-cone” approximation [68]:

$$\frac{dE}{dl d\omega}|_{m_q \neq 0} = \frac{1}{(1 + (\beta\omega)^{3/2})^2} \frac{dE}{dl d\omega}|_{m_q=0}, \quad \beta = \left(\frac{\lambda}{\mu_D^2} \right)^{1/3} \left(\frac{m_q}{E} \right)^{4/3}. \quad (6)$$

One should mention a number of more recent developments in heavy quark energy loss calculations available in the literature (see [8] and references therein), which can be included in the model in the future.

The medium where partonic rescattering occurs is treated as a boost-invariant longitudinally expanding quark-gluon fluid, and the partons as being produced on a hyper-surface of equal proper times τ [69]. In order to simplify numerical calculations we omit here the transverse expansion and viscosity of the fluid using the well-known scaling solution obtained by Bjorken [69] for a temper-

ature T and energy density ε of QGP at $T > T_c \simeq 200$ MeV:

$$\varepsilon(\tau)\tau^{4/3} = \varepsilon_0\tau_0^{4/3}, \quad T(\tau)\tau^{1/3} = T_0\tau_0^{1/3}, \quad \rho(\tau)\tau = \rho_0\tau_0. \quad (7)$$

The proper time τ_0 of QGP formation, the initial QGP temperature T_0 at mid-rapidity ($y = 0$) for central (impact parameter $b = 0$) Pb+Pb collisions, and the number N_f of active flavours are input model parameters. For non-central collisions and for other beam atomic numbers, T_0 is calculated automatically: the initial energy density $\varepsilon_0(b)$ is supposed to be proportional to the ratio of nuclear overlap function $T_{AA}(b)$ to effective transverse area of nuclear overlapping $S_{AA}(b)$ [52]:

$$\varepsilon_0(b) = \varepsilon_0(b=0) \frac{T_{AA}(b)}{T_{AA}(b=0)} \frac{S_{AA}(b=0)}{S_{AA}(b)}, \quad \varepsilon_0(A) = \varepsilon_0(Pb) \left(\frac{A}{207} \right)^{2/3}, \quad (8)$$

$$T_{AA}(b) = \int_0^{2\pi} d\psi \int_0^\infty r dr T_A(r_1) T_A(r_2), \quad S_{AA}(b) = \int_0^{2\pi} d\psi \int_0^{R_{\text{eff}}(b,\psi)} r dr, \quad (9)$$

$$T_A(\mathbf{r}) = A \int \rho_A(\mathbf{r}, z) dz, \quad r_{1,2} = \sqrt{r^2 + \frac{b^2}{4} \pm rb \cos \psi}, \quad (10)$$

$$R_{\text{eff}} = \min \left\{ \sqrt{R_A^2 - \frac{b^2}{4} \sin^2 \psi} + \frac{b}{2} \cos \psi, \sqrt{R_A^2 - \frac{b^2}{4} \sin^2 \psi} - \frac{b}{2} \cos \psi \right\}, \quad (11)$$

where $r_{1,2}(b, r, \psi)$ are the distances between the centres of colliding nuclei and the jet production vertex $V(r \cos \psi, r \sin \psi)$ (r being the distance from the nuclear collision axis to V), $R_{\text{eff}}(b, \psi)$ is the transverse distance from the nuclear collision axis to the effective boundary of nuclear overlapping area in the given azimuthal direction ψ (so that $R_{\text{eff}}(b=0)$ is equal to the nuclear radius $R_A = 1.15A^{1/3}$), $T_A(b)$ is the nuclear thickness functions, and $\rho_A(\mathbf{r}, z)$ is the standard Woods-Saxon nucleon density distribution [70] (see [52] for detailed nuclear geometry explanations). The rapidity dependent spreading of the initial energy density around mid-rapidity $y = 0$ is taken in the Gaussian-like form. The radial profile of the energy density (or the temperature) is also introduced in the parton rescattering model. The transverse energy density in each point inside the nuclear overlapping zone is proportional to the impact-parameter dependent product of two nuclear thickness functions T_A in this point:

$$\varepsilon(r_1, r_2) \propto T_A(r_1) T_A(r_2). \quad (12)$$

Thus, in fact, the input parameter $T_0 \propto \varepsilon_0^{1/4}$ acquires the meaning of an effective (i.e. averaged over the whole nuclear overlapping region) initial temperature in central Pb+Pb collisions.

Note that the other scenarios of QGP space-time evolution for the MC imple-

mentation of the model were also studied. In particular, the influence of the transverse flow, as well as that of the mixed phase at $T = T_c$, on the intensity of jet rescattering (which is a strongly increasing function of T) has been found to be inessential for high initial temperatures $T_0 \gg T_c$. On the contrary, the presence of QGP viscosity slows down the cooling rate, that implies a jet parton spending more time in the hottest regions of the medium. As a result the rescattering intensity increases, i.e., in fact the effective temperature of the medium appears to be higher as compared with the perfect QGP case. We also do not take into account here the probability of jet rescattering in the nuclear matter, because the intensity of this process and the corresponding contribution to the total energy loss are not significant due to much smaller energy density in a “cold” nucleus.

Another important element of the model is the angular spectrum of in-medium gluon radiation. Since the detailed calculation of the angular spectrum of emitted gluons is rather sophisticated, the simple “small-angle” parameterization of the gluon distribution over the emission angle θ was used:

$$\frac{dN^g}{d\theta} \propto \sin \theta \exp \left(-\frac{(\theta - \theta_0)^2}{2\theta_0^2} \right), \quad (13)$$

where $\theta_0 \sim 5^\circ$ is the typical angle of the coherent gluon radiation as estimated in [71]. Two other parameterizations (“wide-angle” $dN^g/d\theta \propto 1/\theta$, and “collinear” $dN^g/d\theta = \delta(\theta)$) are also envisaged.

The model for single hard nucleon-nucleon sub-collision PYQUEN [14] was constructed as a modification of the jet event obtained with the generator of hadron-hadron interactions PYTHIA_6.4 [15]. The event-by-event simulation procedure in PYQUEN includes generation of the initial parton spectra with PYTHIA and production vertexes at given impact parameter, rescattering-by-rescattering simulation of the parton path in a dense zone, radiative and collisional energy loss per rescattering, final hadronization with the Lund string model for hard partons and in-medium emitted gluons. Then the PYQUEN multi-jets generated according to the binomial distribution are included in the hard part of the event. If there is no nuclear shadowing, the mean number of jets produced in AA events at a given impact parameter b is proportional to the mean number of binary NN sub-collisions, $\overline{N_{\text{bin}}} = T_{AA}(b)\sigma_{NN}^{\text{in}}(\sqrt{s})$. In the presence of shadowing, this number is determined as

$$\overline{N_{AA}^{\text{jet}}}(b, \sqrt{s}, p_T^{\text{min}}) = \int_{p_T^{\text{min}}} dp_T^2 \int dy \frac{d\sigma_{NN}^{\text{hard}}(p_T, \sqrt{s})}{dp_T^2 dy} \int_0^{2\pi} d\psi \int_0^\infty r dr T_A(r_1) T_A(r_2) S(r_1, r_2, p_T, y), \quad (14)$$

where $\sigma_{NN}^{\text{in}}(\sqrt{s})$ and $d\sigma_{NN}^{\text{hard}}(p_T, \sqrt{s})/dp_T^2 dy$, calculated with PYTHIA, are the total inelastic non-diffractive NN cross section and the differential cross section of the corresponding hard process in NN collisions (at the same c.m.s. energy, \sqrt{s} , of colliding beams) with the minimum transverse momentum transfer p_T^{min} respectively. The latter is another input parameter of the model. In the HYDJET frameworks, partons produced in (semi)hard processes with the momentum transfer lower than p_T^{min} are considered as being “thermalized”, so their hadronization products are included in the soft part of the event “automatically”. The factor $S \leq 1$ in (14) takes into account the effect of nuclear shadowing on parton distribution functions. It can be written as a product of shadowing factors for both the colliding nuclei as

$$S(r_1, r_2, p_T, y) = S_A^i(x_1, Q^2, r_1) S_A^j(x_2, Q^2, r_2) , \quad (15)$$

where $S_A^{i,j}$ is the ratio of nuclear to nucleon parton distribution functions (normalized by the atomic number) for the parton of type $\{i, j\}$ (light quark or gluon), $x_{1,2}$ are the momentum fractions of the initial partons from the incoming nuclei which participate in the hard scattering characterized by the scale $Q^2 = x_1 x_2 s$, and $r_{1,2}$ are the transverse coordinates of the partons in their respective nuclei, so that $\mathbf{r}_1 + \mathbf{r}_2 = \mathbf{b}$. In HYDJET++, nuclear shadowing corrections are implemented not by modifying the parton showering of single NN collisions in PYTHIA but by correcting of the contribution of initial coherent, multiple scattering in effective way. In fact, this nuclear effect reduces the number of partons in the incoming hadronic wave-function of both the nuclei and thus reduces the total jet production cross section. Since the degree of this reduction depends on the kinematic variables of incoming hard partons, both initial and final parton momentum spectra are modified as a result of nuclear shadowing.

The shadowing corrections are expected to be very significant at LHC energies, where both soft and relatively high- p_T ($\lesssim 15$ GeV/ c) particle production probe the low- x gluon distribution of the target at moderate scales, $Q^2 \sim p_\perp^2$, and are therefore strongly influenced by unitarity effects. In the Glauber-Gribov theory [72], this phenomenon arises from coherent interaction of the projectile fluctuation on the target constituents and is closely related to the diffractive structure function of the nucleon. Due to the factorization theorem for hard processes in QCD, S_A^i describes the modifications of nuclear parton distribution functions (i.e. distributions of quarks and gluons in nuclei), such that

$$f_{i/A}(x, Q^2, b) = f_{i/N}(x, Q^2) S_i(A, b, x, Q^2) . \quad (16)$$

From summation of Pomeron fan diagrams the shadowing factor is found to be $S_A^i = 1/(1 + F^i(x, Q^2)T_A(b))$, where the effective cross section for quarks

and gluon, respectively, is found to be

$$F^i(x, Q^2) = 4\pi \int_x^{0.1} dx_{\mathbb{P}} \Pi(x_{\mathbb{P}}) \begin{cases} \beta \Sigma^{\mathcal{D}}(\beta, Q^2) / \Sigma(x, Q^2) \\ \beta g^{\mathcal{D}}(\beta, Q^2) / g(x, Q^2) \end{cases}, \quad (17)$$

$$\Pi(x_{\mathbb{P}}) = B(x_{\mathbb{P}}) f_{\mathbb{P}}(x_{\mathbb{P}}) F_A^2(-x_{\mathbb{P}}^2 m_N^2), \quad (18)$$

where $\Sigma^{\mathcal{D}}$ and $g^{\mathcal{D}}$ denote the quark-singlet and gluon diffractive parton distribution functions, Σ and g are the normal parton distribution functions, B and $f_{\mathbb{P}}$ are the slope of diffractive distribution and the Pomeron flux factor respectively, F_A is the nuclear form factor. The quark and gluon diffractive distributions are taken from the most recent experimental parameterizations by the H1 Collaboration [73], and the resulting shadowing factors calculated in [16] are implemented in HYDJET and HYDJET++.

2.2 Model for the soft “thermal” hadron production

The soft part of HYDJET++ event is the “thermal” hadronic state generated on the chemical and thermal freeze-out hypersurfaces obtained from a parameterization of relativistic hydrodynamics with preset freeze-out conditions. The detailed description of the physics frameworks of this model can be found in the corresponding papers [17,18]. It is supposed that a hydrodynamic expansion of the fireball ends by a sudden system breakup at given temperature T^{ch} and chemical potentials μ_B, μ_S, μ_Q (baryon number, strangeness and electric charge respectively). In this case, the momentum distribution of the produced hadrons retains the thermal character of the (partially) equilibrated Lorentz invariant distribution function in the fluid element rest frame [74,75]:

$$f_i^{\text{eq}}(p^{*0}; T^{\text{ch}}, \mu_i, \gamma_s) = \frac{g_i}{\gamma_s^{-n_i^s} \exp([p^{*0} - \mu_i]/T^{\text{ch}}) \pm 1}, \quad (19)$$

where p^{*0} is the hadron energy in the fluid element rest frame, $g_i = 2J_i + 1$ is the spin degeneracy factor, $\gamma_s \leq 1$ is the (optional) strangeness suppression factor, n_i^s is the number of strange quarks and antiquarks in a hadron i . The signs \pm in the denominator account for the quantum statistics of a fermion or a boson, respectively. Then the particle number density $\rho_i^{\text{eq}}(T, \mu_i)$ can be represented in the form of a fast converging series [17], that is,

$$\rho_i^{\text{eq}}(T, \mu_i) = \frac{g_i}{2\pi^2} m_i^2 T \sum_{k=1}^{\infty} \frac{(\mp)^{k+1}}{k} \exp\left(\frac{k\mu_i}{T}\right) K_2\left(\frac{km_i}{T}\right), \quad (20)$$

where K_2 is the modified Bessel function of the second order and m_i is the particle mass.

The mean multiplicity \bar{N}_i of a hadron species i crossing the space-like freeze-out hypersurface $\sigma(x)$ in Minkowski space is computed using effective thermal volume approximation [76,77]:

$$\bar{N}_i = \rho_i^{\text{eq}}(T, \mu_i) \int_{\sigma(x)} d^3\sigma_\mu(x) u^\mu(x) = \rho_i^{\text{eq}}(T, \mu_i) V_{\text{eff}} , \quad (21)$$

where the four-vector $d^3\sigma_\mu(x) = n_\mu(x) d^3\sigma(x)$ is the element of the freeze-out hypersurface directed along the hypersurface normal unit four-vector $n^\mu(x)$ with a positively defined zero component ($n^0(x) > 0$), $d^3\sigma(x) = |d^3\sigma_\mu d^3\sigma^\mu|^{1/2}$ is the invariant measure of this element. The probability that the produced grand canonical ensemble consists of N_i particles is thus given by Poisson distribution around its mean value \bar{N}_i :

$$P(N_i) = \exp(-\bar{N}_i) \frac{(\bar{N}_i)^{N_i}}{N_i!} . \quad (22)$$

The chemical potential μ_i for any particle species i at the chemical freeze-out is entirely determined by chemical potentials $\tilde{\mu}_q$ per unit charge, i.e., per unit baryon number B , strangeness S , electric charge (isospin) Q , charm C , etc. It can be expressed as a scalar product, $\mu_i = \vec{q}_i \tilde{\mu}$, where $\vec{q}_i = \{B_i, S_i, Q_i, C_i, \dots\}$ and $\tilde{\mu} = \{\tilde{\mu}_B, \tilde{\mu}_S, \tilde{\mu}_Q, \tilde{\mu}_C, \dots\}$. Assuming constant temperature and chemical potentials on the chemical freeze-out hypersurface, the total quantum numbers $\vec{q} = \{B, S, Q, C, \dots\}$ of the thermal part of produced hadronic system with corresponding V_{eff} can be calculated as $\vec{q} = V_{\text{eff}} \sum_i \rho_i^{\text{eq}} \vec{q}_i$. Thus, the potentials $\tilde{\mu}_q$ are not independent, so taking into account baryon, strangeness and electrical charges only and fixing the total strangeness S and the total electric charge Q , $\tilde{\mu}_S$ and $\tilde{\mu}_Q$ can be expressed through baryonic potential $\tilde{\mu}_B$. Therefore, the mean number of each particle and resonance species at chemical freeze-out is determined solely by the temperature T and the baryonic chemical potential $\tilde{\mu}_B$, which can be related within the thermal statistical approach using the following parameterization [78]:

$$T(\tilde{\mu}_B) = a - b\tilde{\mu}_B^2 - c\tilde{\mu}_B^4 , \quad \tilde{\mu}_B(\sqrt{s}_{NN}) = \frac{d}{1 + e\sqrt{s}_{NN}} , \quad (23)$$

where $a = 0.166 \pm 0.002$ GeV, $b = 0.139 \pm 0.016$ GeV⁻¹, $c = 0.053 \pm 0.021$ GeV⁻³ and $d = 1.308 \pm 0.028$ GeV, $e = 0.273 \pm 0.008$ GeV⁻¹.

Since the particle densities at the chemical freeze-out stage may be too high to consider the particles as free streaming (see, e.g., [79]), the assumption of the common chemical and thermal freeze-outs can hardly be justified, so a more complicated scenario with different chemical and thermal freeze-outs is implemented in HYDJET++ ($T^{\text{ch}} \geq T^{\text{th}}$). Within the concept of chemically frozen evolution, particle numbers are assumed to be conserved except for corrections due to decay of some part of the short-lived resonances that can be estimated from the assumed chemical to thermal freeze-out evolution time.

Then to determine the particle densities $\rho_i^{\text{eq}}(T^{\text{th}}, \mu_i^{\text{th}})$ at the temperature of thermal freeze-out T^{th} , the conservation of the particle fractions from the chemical to thermal freeze-out evolution time is supposed, and an additional input model parameter, effective pion chemical potential $\mu_\pi^{\text{eff th}}$ at thermal freeze-out, is introduced:

$$\frac{\rho_i^{\text{eq}}(T^{\text{ch}}, \mu_i)}{\rho_\pi^{\text{eq}}(T^{\text{ch}}, \mu_i^{\text{ch}})} = \frac{\rho_i^{\text{eq}}(T^{\text{th}}, \mu_i^{\text{th}})}{\rho_\pi^{\text{eq}}(T^{\text{th}}, \mu_\pi^{\text{eff th}})} . \quad (24)$$

Assuming for the particles heavier than pions the Boltzmann approximation in (20), one deduces from (20) and (24) the chemical potentials of hadrons at thermal freeze-out:

$$\mu_i^{\text{th}} = T^{\text{th}} \ln \left(\frac{\rho_i^{\text{eq}}(T^{\text{ch}}, \mu_i^{\text{ch}})}{\rho_i^{\text{eq}}(T^{\text{th}}, \mu_i = 0)} \frac{\rho_\pi^{\text{eq}}(T^{\text{th}}, \mu_\pi^{\text{eff th}})}{\rho_\pi^{\text{eq}}(T^{\text{ch}}, \mu_i^{\text{ch}})} \right) . \quad (25)$$

Note that it can no longer be expressed in the form $\mu_i = \vec{q}_i \vec{\tilde{\mu}}$, which is valid only for chemically equilibrating systems.

At relativistic energies, because of the dominant longitudinal motion, it is convenient to parameterize the fluid flow four-velocity $\{u^0(x), \vec{u}(x)\} = \gamma\{1, \vec{v}(x)\}$ at a point x in terms of the longitudinal (z) and transverse (r_\perp) fluid flow rapidities

$$\eta^u(x) = \frac{1}{2} \ln \frac{1 + v_z(x)}{1 - v_z(x)}, \quad \rho^u(x) = \frac{1}{2} \ln \frac{1 + v_\perp(x) \cosh \eta^u(x)}{1 - v_\perp(x) \cosh \eta^u(x)}, \quad (26)$$

where $v_\perp = |\vec{v}_\perp|$ is the magnitude of the transverse component of the flow three-velocity $\vec{v} = \{\vec{v}_\perp, v_z\} = \{v_\perp \cos \phi^u, v_\perp \sin \phi^u, v_z\}$, i.e.,

$$\begin{aligned} u^\mu(x) &= \{\cosh \rho^u \cosh \eta^u, \sinh \rho^u \cos \phi^u, \sinh \rho^u \sin \phi^u, \cosh \rho^u \sinh \eta^u\} \\ &= \{(1 + u_\perp^2)^{1/2} \cosh \eta^u, \vec{u}_\perp, (1 + u_\perp^2)^{1/2} \sinh \eta^u\} , \end{aligned} \quad (27)$$

$\vec{u}_\perp = \gamma \vec{v}_\perp = \cosh \eta^u \gamma_\perp \vec{v}_\perp$, $\gamma_\perp = \cosh \rho^u$. The linear transverse rapidity profile is used and the momentum anisotropy parameter $\delta(b)$ is introduced here:

$$\begin{aligned} u^x &= \sqrt{1 + \delta(b)} \sinh \tilde{\rho}_u \cos \phi, \quad u^y = \sqrt{1 - \delta(b)} \sinh \tilde{\rho}_u \sin \phi, \\ \tilde{\rho}_u &= \frac{r}{R_f(b)} \rho_u^{\text{max}}(b=0), \end{aligned} \quad (28)$$

where ϕ is the spatial azimuthal angle of the fluid element, r is its radial coordinate, $\rho_u^{\text{max}}(b=0)$ is the maximal transverse flow rapidity for central collisions, and $R_f(b)$ is the mean-square radius of the hadron emission region [18], which determines the fireball transverse radius $R(b, \phi)$ in the given

azimuthal direction ϕ through the spatial anisotropy parameter $\epsilon(b)$:

$$R(b, \phi) = R_f(b) \frac{\sqrt{1 - \epsilon^2(b)}}{\sqrt{1 + \epsilon(b) \cos 2\phi}}. \quad (29)$$

For this case, it is straightforward to derive the formula for the total effective volume of hadron emission from the hypersurface of proper time $\tau = \text{const}$ [17,18]:

$$V_{\text{eff}} = \int_{\sigma(t, \vec{x})} d^3\sigma_\mu(t, \vec{x}) u^\mu(t, \vec{x}) = \tau \int_0^{2\pi} d\phi \int_0^{R(b, \phi)} (n_\mu u^\mu) r dr \int_{\eta_{\min}}^{\eta_{\max}} f(\eta) d\eta, \quad (30)$$

where $(n_\mu u^\mu) = \cosh \tilde{\rho}_u \sqrt{1 + \delta(b) \tanh^2 \tilde{\rho}_u \cos 2\phi}$, and $f(\eta)$ is the longitudinal flow rapidity profile (Gaussian or uniform).

The value V_{eff} is calculated in HYDJET++ only for central collisions ($b = 0$), and then for non-central collisions it is supposed to be proportional to the mean number of nucleons-participants $\overline{N_{\text{part}}}(b)$ (39):

$$V_{\text{eff}}(b) = V_{\text{eff}}(b = 0) \frac{\overline{N_{\text{part}}}(b)}{\overline{N_{\text{part}}}(b = 0)}. \quad (31)$$

Since the fireball transverse radius $R_f(b = 0)$ and the freeze-out proper time $\tau_f(b = 0)$ (as well as its standard deviation $\Delta\tau_f(b = 0)$ – the emission duration) are the input model parameters, it is straightforward to determine these values for non-central collisions through the effective volume V_{eff} and input anisotropy parameters ϵ and δ at the given b :

$$R_f(b) = R_f(0) \left(\frac{V_{\text{eff}}[R_f(0), \tau_f(0), \epsilon(0), \delta(0)]}{V_{\text{eff}}[R_f(0), \tau_f(0), \epsilon(b), \delta(b)]} \right)^{1/2} \left(\frac{\overline{N_{\text{part}}}(b)}{\overline{N_{\text{part}}}(b = 0)} \right)^{1/3}, \quad (32)$$

$$\tau_f(b) = \tau_f(0) \left(\frac{\overline{N_{\text{part}}}(b)}{\overline{N_{\text{part}}}(b = 0)} \right)^{1/3}, \quad \Delta\tau_f(b) = \Delta\tau_f(0) \left(\frac{\overline{N_{\text{part}}}(b)}{\overline{N_{\text{part}}}(b = 0)} \right)^{1/3} \quad (33)$$

Note that such choice of centrality dependence for $R_f(b)$ and $\tau_f(b)$ is inspired by the experimentally observed dependence of momentum correlation radii $R_{\text{side}}(b)$, $R_{\text{out}}(b)$, $R_{\text{long}}(b) \propto N_{\text{part}}(b)^{1/3}$ [80,81]. The detailed study of femtoscopic momentum correlations at RHIC and LHC (including their centrality dependence) is planned in the HYDJET++ frameworks for the future.

The momentum and spatial anisotropy parameters $\delta(b)$ and $\epsilon(b)$ can be treated independently for each centrality, or can be related to each other through the dependence of the elliptic flow coefficient $v_2(\epsilon, \delta)$ (the second-order Fourier coefficient in the hadron distribution over the azimuthal angle φ relatively to

the reaction plane) obtained in the hydrodynamical approach [82]:

$$v_2 \propto \frac{2(\delta - \epsilon)}{(1 - \delta^2)(1 - \epsilon^2)} . \quad (34)$$

Then using the predicted by hydrodynamical models (and observed at RHIC) proportionality of the value $v_2(b)$ and the initial ellipticity $\epsilon_0(b) = b/2R_A$ (i.e. $v_2 \propto \epsilon_0$), one can derive the relation between $\delta(b)$ and $\epsilon(b)$ (supposing also $\epsilon \propto \epsilon_0$):

$$\delta = \frac{\sqrt{1 + 4B(\epsilon + B)} - 1}{2B} , \quad B = C(1 - \epsilon^2)\epsilon , \quad \epsilon = k\epsilon_0, \quad (35)$$

where C and k are the independent on centrality coefficients, which should be specified instead of $\delta(b)$ and $\epsilon(b)$ dependences. The best fit of RHIC data to the elliptic flow (Figure 6 in Section 6) is obtained with the values $C = 2$ and $k = 0.175$.

The “thermal” hadronic state in HYDJET++ consists of stable hadrons and resonances produced from the SHARE particle data table [19], which contains 360 particles (excluding any not well established resonance states). The decays of resonances are controlled by the decay lifetime $1/\Gamma$, where Γ is the resonance width specified in the particle table, and these decays occur with the probability density $\Gamma \exp(-\Gamma\tau)$ in the resonance rest frame. Then the decay products are boosted to the reference frame in which the freeze-out hypersurface was defined. The space-time coordinates of the decaying particle are shifted from its initial position on the decay length $\Delta\tau P/M$ (M and P are the decaying particle mass and four-momenta respectively). The branching ratios are also taken from the SHARE [19]. Only the two- and three-body decays are taken into account in the model. The cascade decays are also possible. Resonances are given the mass distribution according to a non-relativistic Breit-Wigner

$$P(m)dm \propto \frac{1}{(m - m_0)^2 + \Delta m^2/4} dm, \quad (36)$$

where m_0 and Δm are the resonance nominal mass and width respectively. The Breit-Wigner shape is truncated symmetrically, $|m - m_0| < \Delta m$, with Δm taken for each particle from the PYTHIA [15] ($\Delta m = 0$ for some narrow resonances which are not present in PYTHIA).

3 Simulation procedure

Before any event generation, HYDJET++ run starts from PYTHIA initialization at the given c.m.s. energy per nucleon pair \sqrt{s} (input parameter `fSqrtS`),

and then it calculates the total inelastic NN cross section $\sigma_{NN}^{\text{in}}(\sqrt{s})$ (output parameter **Sigin**) and the hard scattering NN cross section $\sigma_{NN}^{\text{hard}}(\sqrt{s}, p_T^{\text{min}})$ (output parameter **Sigjet**) with the minimum transverse momentum transfer p_T^{min} (input parameter **fPtm**). Then the tabulation of nuclear thickness function $T_A(b)$ and nuclear overlap function $T_{AA}(b)$ is performed. If the impact parameter b of heavy ion AA collision is not fixed (input parameter **fIfb** $\neq 0$), its value b (output parameter **Bgen**) is generated in each event between the minimum (input parameter **fBmin**) and maximum (input parameter **fBmax**) values in accordance with the differential inelastic AA cross section, obtained from the standard generalization of Glauber multiple scattering model [83] to the case of independent inelastic nucleon-nucleon collisions:

$$\frac{d^2\sigma_{\text{in}}^{AA}}{d^2b}(b, \sqrt{s}) = \left[1 - \left(1 - \frac{1}{A^2} T_{AA}(b) \sigma_{NN}^{\text{in}}(\sqrt{s}) \right)^{A^2} \right] . \quad (37)$$

If the impact parameter b is fixed (**fIfb** = 0), then its value **Bgen** in each event is equal to the input parameter **fBfix**. After specification of b for each given event, the mean numbers of binary NN sub-collisions $\overline{N_{\text{bin}}}$ (output parameter **Nbcol**) and nucleons-participants $\overline{N_{\text{part}}}$ (output parameter **Npart**) are calculated:

$$\overline{N_{\text{bin}}}(b, \sqrt{s}) = T_{AA}(b) \sigma_{NN}^{\text{in}}(\sqrt{s}) , \quad (38)$$

$$\overline{N_{\text{part}}}(b, \sqrt{s}) = \int_0^{2\pi} d\psi \int_0^\infty r dr T_A(r_1) \left[1 - \exp \{ \sigma_{NN}^{\text{in}}(\sqrt{s}) T_A(r_2) \} \right] . \quad (39)$$

The next step is the simulation of particle production proper in the event. The soft, hydro-type state and the hard, multi-jet state are simulated independently. When the generation of soft and hard states in each event at given b is completed, the event record (information about coordinates and momenta of initial particles, decay products of unstable and stable particles) is formed as the junction of these two independent event outputs in the **RunOutput.root** file.

3.1 Generation of the hard multi-jet state

The following event-by-event MC simulation procedure is applied to generate the hard state resulting from multi-parton fragmentation in the case when jet production is switched on (input parameter **fNhse1**=1, 2, 3 or 4).

- (1) Calculation of the number of NN sub-collisions N_{AA}^{jet} (output parameter **Njet**) producing hard parton-parton scatterings of selected type (QCD-dijets by default, PYTHIA parameter **msel**=1) with $p_T > p_T^{\text{min}}$, according

to the binomial distribution around its mean value (14) (without shadowing correction yet, $S = 1$). For this purpose, each of `Nbcol` sub-collisions is tested basing on comparison of random number ξ_i generated uniformly in the interval $[0, 1]$ with the probability `pjet=Sigjet/Sigin` to produce the hard process. The i -th sub-collision is accepted if $\xi_i < \text{pjet}$, and is rejected in the opposite case.

- (2) Selecting the type of hard NN sub-collision (pp, np or nn) in accordance with the phenomenological formula for the number of protons Z in the stable nucleus A , $Z = A/(1.98+0.015A^{2/3})$. For this purpose, each of `Njet` “successful” sub-collisions is tested basing on comparison of two random numbers ξ_i^1 and ξ_i^2 generated uniformly in the interval $[0, 1]$ with the probability Z/A . The proton-proton sub-collision is selected if $\xi_i^1, \xi_i^2 < Z/A$, neutron-neutron sub-collision — if $\xi_i^1, \xi_i^2 > Z/A$, and proton-neutron sub-collision — in other cases.
- (3) Generation of multi-parton production in `Njet` hard NN sub-collisions by calling PYTHIA `Njet` times (`call_pyinit` and `call_pyevnt`, parton fragmentation being switched off by setting `mstp(111)=0`). The spatial vertex of jet production for each sub-collision is generated by PYQUEN routine according to the distribution

$$\frac{dN^{\text{jet}}}{d\psi r dr}(b) = \frac{T_A(r_1) \cdot T_A(r_2)}{T_{AA}(b)} . \quad (40)$$

- (4) If jet quenching is switched on (`fNhse1=2` or `4`), initial PYTHIA-produced partonic state is modified by QCD-medium effects with PYQUEN generator for each sub-collision separately. The radiative and collisional energy loss are both taken into account by default (input parameter `fIengl=0`), but the options to have only radiative loss (`fIengl=1`) or only collisional loss (`fIengl=2`) are envisaged. For each hard parton with the initial transverse momentum $p_T > 3$ GeV/ c and pseudorapidity $|\eta| < 3.5$ in the given sub-collision, the following rescattering scheme is applied.

- Calculation of the scattering cross section $\sigma(\tau_i) = \int dt d\sigma/dt$ and generation of the transverse momentum transfer $t(\tau_i)$ in the i -th scattering according to (3) (τ_i is a current proper time).
- Generation of the displacement between the i -th and $(i+1)$ -th scatterings, $l_i = (\tau_{i+1} - \tau_i)$:

$$\frac{dP}{dl_i} = \lambda^{-1}(\tau_{i+1}) \exp\left(-\int_0^{l_i} \lambda^{-1}(\tau_i + s) ds\right), \quad \lambda^{-1}(\tau) = \sigma(\tau)\rho(\tau), \quad (41)$$

and calculation of the corresponding transverse distance, $l_i p_T / E$.

- Generation of the energy of a radiated in the i -th scattering gluon, $\omega_i = \Delta E_{\text{rad},i}$, according to (4) and (6):

$$\frac{dI}{d\omega}|_{m_q=0} = \frac{2\alpha_s(\mu_D^2)\lambda C_R}{\pi L\omega} \left[1 - y + \frac{y^2}{2} \right] \ln |\cos(\omega_1\tau_1)| , \quad (42)$$

$$\frac{dI}{d\omega}|_{m_q \neq 0} = \frac{1}{(1 + (\beta\omega)^{3/2})^2} \frac{dI}{d\omega}|_{m_q=0} , \quad (43)$$

and its emission angle θ_i relative to the parent parton determined according to the small-angle distribution (13) (input parameter `fIanglu=0`). The options to have wide-angle (`fIanglu=1`) or collinear (`fIanglu=2`) distributions are also envisaged.

- Calculation of the collisional energy loss in the i -th scattering

$$\Delta E_{\text{col},i} = \frac{t_i}{2m_0} , \quad (44)$$

where energy of “thermal” medium parton m_0 is generated according to the isotropic Boltzmann distribution at the temperature $T(\tau_i)$.

- Reducing the parton energy by collisional and radiative loss per each i -th scattering,

$$\Delta E_{\text{tot},i} = \Delta E_{\text{col},i} + \Delta E_{\text{rad},i} , \quad (45)$$

and changing the parton momentum direction by means of adding the transverse momentum recoil due to elastic scattering i ,

$$\Delta k_{t,i}^2 = (E - \frac{t_i}{2m_{0i}})^2 - (p - \frac{E}{p} \frac{t_i}{2m_{0i}} - \frac{t_i}{2p})^2 - m_p^2 . \quad (46)$$

- Going to the next rescattering, or halting the rescattering if one of the following two conditions is fulfilled: (a) the parton escapes the hot QGP zone, i.e. the temperature in the next point $T(\tau_{i+1}, r_{i+1}, \eta_{i+1})$ becomes lower than $T_c = 200$ MeV; or (b) the parton loses so much of energy that its transverse momentum $p_T(\tau_{i+1})$ drops below the average transverse momentum of the “thermal” constituents of the medium, $2T(\tau_{i+1})$. In the latter case, such a parton is considered to be “thermalized” and its momentum in the rest frame of the quark-gluon fluid is generated from the random “thermal” distribution, $dN/d^3p \propto \exp(-E/T)$, boosted to the center-of-mass of the nucleus-nucleus collision.

At the end of each NN sub-collision, adding new (in-medium emitted) gluons to the PYTHIA parton list and rearrangement of partons to update string formation with the subroutine PYJOIN are performed. An additional gluon is included in the same string as its “parent”, and colour connections of such gluons are re-ordered relative to their z -coordinates along the string.

- (5) If the nuclear shadowing is switched on (input parameter `fIshad=1`) and beam ions are Pb, Au, Pd or Ca (`fAw=207.`, `197.`, `110.` or `40.`), each hard NN sub-collision is tested basing on comparison of random number ξ_i generated uniformly in the interval $[0, 1]$ with the shadowing factor S

(15) taken from the available parameterization (`subroutine_eggshad`). It is determined by the type of initially scattered hard partons, momentum fractions obtained by the partons at the initial hard interaction $x_{1,2}$ (PYTHIA parameters `pari(33)`, `pari(34)`), the square of transverse momentum transfer in the hard scattering Q^2 (PYTHIA parameter `pari(22)`), and the transverse position of jet production vertex relative to the centres of nuclei $r_{1,2}$. The given sub-collision is accepted if $\xi_i < S$, and is rejected in the opposite case.

- (6) Formation of hadrons for each “accepted” hard NN sub-collision with PYTHIA (parton fragmentation being switched on by `call_pyexec`), and final junction of `Njet` sub-events to common array `hyjets` using standard PYTHIA event output format. If particle decays in PYTHIA are switched off (input PYTHIA parameter `mstj(21)=0`), then formation of final hadrons from the two- and three-body decays of resonances follows the same pattern as that for soft hydro-part with the branching ratios taken from the SHARE particle decay table [19].

3.2 Generation of the soft “thermal” state

The following event-by-event MC simulation procedure is applied to generate the soft “thermal” state in the case when soft hadroproduction is switched on (input parameter `fNhse1=0, 1, or 2`).

- (1) Initialization of the chemical freeze-out parameters. It includes the calculation of particle number densities according to (20) (the calculation of chemical freeze-out temperature, baryon potential and strangeness potential as a function of beam c.m.s. energy `fSqrtS` according to (23) is performed in advance if the corresponding flag `fTMuType>0`). So far, only the stable hadrons and resonances consisting of u , d , s quarks are taken into account from the SHARE particle data table [19].
- (2) Initialization of the thermal freeze-out parameters (if $T^{\text{th}} < T^{\text{ch}}$). It includes the calculation of chemical potentials according to (25) and particle number densities according to (24).
- (3) Calculation of the effective volume of hadron emission region $V_{\text{eff}}(b)$ according to (31) and (30), the fireball transverse radius $R_f(b)$, the freeze-out proper time $\tau_f(b)$ and the emission duration $\Delta\tau_f(b)$ according to (32) and (33), and the mean multiplicity of each particle species according to (21). Then the multiplicity is generated around its mean value according to the Poisson distribution (24).
- (4) For each hadron the following procedure to generate its four-momentum is applied (resonance mass is generated according to (36)).

- Generation of four-coordinates of a hadron in the fireball rest frame $x^\mu = \{\tau \cosh \eta, r \cos \phi, r \sin \phi, \tau \sinh \eta\}$ on each freeze-out hypersurface segment $\tau(r)$ for the element $d^3\sigma_\mu u^\mu = d^3\sigma_0^* = n_0^*(r) |1 - (d\tau/dr)^2|^{1/2} \tau(r) d^2r d\eta$, assuming n_0^* and τ to be the functions of r (i.e., independent of η, ϕ). It includes sampling uniformly distributed ϕ in the interval $[0, 2\pi]$, generating η according to the uniform distribution in the interval $[-\eta_{\max}, \eta_{\max}]$ (if flag `fEtaType` ≤ 0) or Gaussian distribution $\exp(-\eta^2/2\eta_{\max}^2)$ (if flag `fEtaType` > 0) and r in the interval $[0, R_f(b)]$ using a 100% efficient procedure similar to the ROOT routine `GetRandom()`.
- Calculation of the corresponding collective flow four-velocities according to (27) and (28).
- Generation of the three-momentum of a hadron in the fluid element rest frame $p^* \{\sin \theta_p^* \cos \phi_p^*, \sin \theta_p^* \sin \phi_p^*, \cos \theta_p^*\}$ according to the equilibrium distribution function $f_i^{\text{eq}}(p^{0*}; T, \mu_i) p^{*2} dp^* d \cos \theta_p^* d \phi_p^*$ by means of sampling uniformly distributed $\cos \theta_p^*$ in the interval $[-1, 1]$ and ϕ_p^* in the interval $[0, 2\pi]$, and generating p^* using a 100% efficient procedure (similar to ROOT routine `GetRandom()`).
- The standard von Neumann rejection/acceptance procedure to take into account the difference between the true probability $W_{\sigma,i}^* d^3\sigma d^3\vec{p}^*/p^{0*}$ and the probability $n^{0*} f_i^{\text{eq}}(p^{0*}; T, \mu_i) d^2r d\eta d^3\vec{p}^*$ corresponding to the previous simulation steps. For this purpose, the residual weight is calculated [17]:

$$W_i^{\text{res}} = \frac{W_{\sigma,i}^* d^3\sigma}{n^{0*} p^{0*} f_i^{\text{eq}} d^2r d\eta} = \tau \left(1 - \frac{\vec{n}^* \vec{p}^*}{n^{0*} p^{0*}} \right). \quad (47)$$

Then the simulated hadron four-coordinate and four-momentum is tested basing on comparison of W_i^{res} with the random number ξ_i generated uniformly in the interval $[0, \max(W_i^{\text{res}})]$. The i -th hadron is accepted if $\xi_i < W_i^{\text{res}}$, and rejected in the opposite case (then the generation of its four-coordinate and four-momentum is repeated).

- Boost of the hadron four-momentum in the center mass frame of the event using the velocity field $\vec{v}(x)$, that is,

$$p^0 = \gamma(p^{0*} + \vec{v} \vec{p}^*), \quad \vec{p} = \vec{p}^* + \gamma(1 + \gamma)^{-1}(p^{0*} + p^0) \vec{v}. \quad (48)$$

Note that the high generation speed for this algorithm is achieved due to almost 100% generation efficiency because of nearly uniform residual weights W_i^{res} (47).

- (5) Formation of final hadrons from the two- and three-body decays of resonances with the random choice of decay channel according to the branching ratios taken from the particle data file `tabledecay.txt` (by default, if flags `fDecay` and `fWeakDecay` ≥ 0). The particle “decay” programs developed by N.S. Amelin for FAST MC generator [17,18] are implemented in HYDJET++.
- For the two-body decay, the momenta $|p_{1,2}|$ of decay products in the

resonance rest frame is calculated as:

$$|p_{1,2}| = 0.5\sqrt{((M^2 - m_1^2 - m_2^2)^2 - 4m_1^2m_2^2)}/M, \quad (49)$$

where M is the resonance mass, and $m_{1,2}$ are the decay product masses. The space orientation of the $|p_{1,2}|$ is generated randomly by sampling uniformly distributed cosine of the polar angle $\cos(\theta)$ in the interval $[-1, 1]$ and the azimuthal angle ϕ in the interval $[0, 2\pi]$ (in the resonance rest frame). The opposite directions for $p_{1,2}$ vectors are chosen according to momentum conservation law.

- For the three-body decay, the resonance energy is divided between the kinetic energy of three decay products uniformly (assuming constant matrix element of the decay):

$$\begin{aligned} E_1^{\text{kin}} &= \xi_1 \Delta M, & |p_1| &= \sqrt{((E_1^{\text{kin}})^2 + 2E_1^{\text{kin}}m_1)} \\ E_2^{\text{kin}} &= (1 - \xi_2) \Delta M, & |p_2| &= \sqrt{((E_2^{\text{kin}})^2 + 2E_2^{\text{kin}}m_2)} \\ E_3^{\text{kin}} &= (\xi_2 - \xi_1) \Delta M, & |p_3| &= \sqrt{((E_3^{\text{kin}})^2 + 2E_3^{\text{kin}}m_3)}, \end{aligned}$$

where ξ_1 and ξ_2 are the two random numbers distributed uniformly in the interval $[0, 1]$ under the condition $\xi_2 > \xi_1$, and $\Delta M = M - m_1 - m_2 - m_3$. For the first particle, the space orientation of the $|p_1|$ is generated randomly by sampling uniformly distributed $\cos(\theta)$ in the interval $[-1, 1]$ and ϕ in the interval $[0, 2\pi]$ (in the resonance rest frame). Then the three-momenta of remaining two particles are calculated taking into account complanarity of the decay and the conservation laws:

$$\begin{aligned} p_2^X &= |p_2| (\sin \theta_N \cos \phi_N \cos \theta \cos \phi - \sin \theta_N \sin \phi_N \sin \phi + \cos \theta_N \sin \theta \cos \phi), \\ p_2^Y &= |p_2| (\sin \theta_N \cos \phi_N \cos \theta \sin \phi - \sin \theta_N \sin \phi_N \cos \phi + \cos \theta_N \sin \theta \sin \phi), \\ p_2^Z &= |p_2| (-\sin \theta_N \cos \phi_N \sin \theta + \cos \theta_N \cos \theta), \\ \vec{p}_3 &= -(\vec{p}_2 + \vec{p}_1), \\ \cos \theta_N &= (|p_2|^2 - |p_3|^2 - |p_1|^2)/(2|p_1||p_3|), \end{aligned}$$

and ϕ_N is generated uniformly in the interval $[0, 2\pi]$. Finally, the momenta of decay particles for two- and three-body decays are boosted to the center-of-mass of the nucleus-nucleus collision with the resonance velocity. The space-time coordinates of the decay products coincide with the coordinates of decay of the initial resonance.

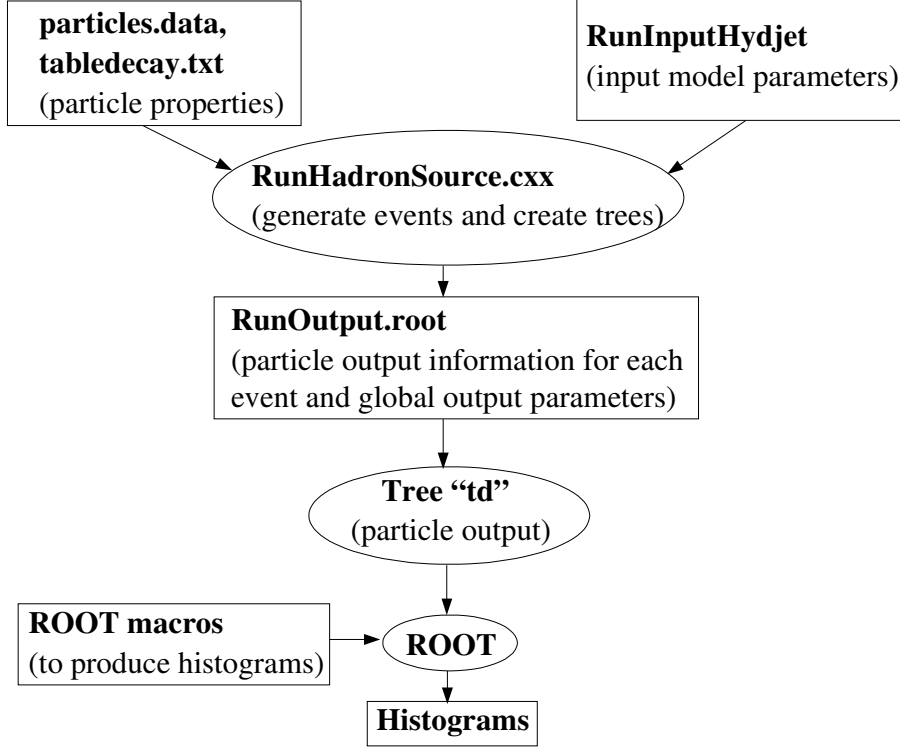


Fig. 1. The block structure of **Hydjet++**.

4 Overview of **HYDJET++** software structure

The basic frameworks of **HYDJET++** are preset by the object-oriented C++ language and the ROOT environment [1]. There is also the Fortran-written part [13] which is included in the generator structure as a separate directory. The block structure of **HYDJET++** is shown in Figure 1. The main program elements (particle data files, input and output files, C++ and Fortran routines) are described in details in this section below.

4.1 Particle data files

The information regarding the particle species included in the soft part of the **HYDJET++** event is stored in the files **particles.data** and **tabledecay.txt**. The **particles.data** file contains the definition (PDG code) and physical properties (mass, decay width, spin, isospin, valence quark composition) of 360 stable hadrons and resonances. The **tabledecay.txt** file contains decay channels and branching ratios. The structure of these files is the same as that in SHARE particle data table [19] and in event generator THERMINATOR [37], where the corresponding description in more details can be found.

The file **particles.data** has the following format.

name – the particle label;
mass – mass in GeV/c^2 ;
width – width in GeV/c^2 ;
spin – spin;
I – isospin;
I3 – third component of isospin;
q – number of light valence quarks in the particle;
s – number of strange valence quarks in the particle;
aq – number of light valence antiquarks in the particle;
as – number of strange valence antiquarks in the particle;
c – number of charm valence quarks in the particle;
ac – number of charm valence antiquarks in the particle;
MC – the particle identification code.

The file **tabledecay.txt** has the following format.

PdgParent – parent particle code;
PdgDaughter1 – first particle (decay product) code;
PdgDaughter2 – second particle (decay product) code;
PdgDaughter3 – third particle (decay product) code (appears for the three-body decays only);
BR – the branching ratio for the decay.

Note that the default PYTHIA_6.4 particle data settings [15] are used to generate hard part of HYDJET++ event.

4.2 *Input parameters and files*

Run of HYDJET++ is controlled by the file **RunInputHydjet** for different type of input parameters. For current version of the generator, two additional files with the optimized parameters for Au+Au collisions at $\sqrt{s} = 200A$ GeV (**RunInputHydjetRHIC200**, Fig. 2) and for Pb+Pb collisions at $\sqrt{s} = 5500A$ GeV (**RunInputHydjetLHC5500**, Fig. 3) are available. To use them as the input one, the user should change the name of the corresponding file to the **RunInputHydjet**. The default parameters for **RunInputHydjetRHIC200** were obtained by fitting RHIC data to various physical observables (see Section 6 for the details). The default parameters for **RunInputHydjetLHC5500** represent our rough extrapolation from RHIC to LHC energy, and of course they may be varied freely by the user.

The following input parameters should be specified by the user.

fNevnt – number of events to generate;
fSqrtS – beam c.m.s. energy per nucleon pair in GeV;

fAw – atomic weight of nuclei;
fIfb – flag of type of centrality generation (=0: impact parameter is fixed by **fBfix** value, $\neq 0$: impact parameter is generated in each event between minimum (**fBmin**) and maximum (**fBmax**) values according to the distribution (37));
fBmin – minimum impact parameter in units of nucleus radius R_A ;
fBmax – maximum impact parameter in units of nucleus radius R_A ;
fBfix – fixed impact parameter in units of nucleus radius R_A .

The following input parameters may be changed by user from their default values.

fSeed – parameter to set the random number seed (=0: the current time is used to set the random generator seed, $\neq 0$: the value **fSeed** is used to set the random generator seed and then the state of random number generator in PYTHIA is **MRPY(1)=fSeed**) (default: 0).

Parameters for soft hydro-type part of the event.

fT – chemical freeze-out temperature T^{ch} in GeV;
fMuB – chemical baryon potential per unit charge $\widetilde{\mu}_B$ in GeV;
fMuS – chemical strangeness potential per unit charge $\widetilde{\mu}_S$ in GeV;
fMuI3 – chemical isospin potential per unit charge $\widetilde{\mu}_Q$ in GeV;
fTthF0 – thermal freeze-out temperature T^{th} in GeV;
fMu_th_pip – chemical potential of positively charged pions at thermal freeze-out $\mu_{\pi}^{\text{eff th}}$ in GeV;
fTau – proper time at thermal freeze-out for central collisions $\tau_f(b=0)$ in fm/c;
fSigmaTau – duration of emission at thermal freeze-out for central collisions $\Delta\tau_f(b=0)$ in fm/c;
fR – maximal transverse radius at thermal freeze-out for central collisions $R_f(b=0)$ in fm;
fYlmax – maximal longitudinal flow rapidity at thermal freeze-out η_{max} ;
fUmax – maximal transverse flow rapidity at thermal freeze-out for central collisions $\rho_u^{\text{max}}(b=0)$;
fDelta – momentum azimuthal anisotropy parameter at thermal freeze-out δ (for given event centrality class);
fEpsilon – coordinate azimuthal anisotropy parameter at thermal freeze-out ϵ (for given event centrality class);
fIfDeltaEpsilon – flag to use calculated δ and ϵ (≤ 0 : specified by user values for given event centrality class are taken, > 0 : calculated for given impact parameter according to the parameterization (35) values are used in each event) (default: 0);
fDecay – flag to switch on/off hadron decays (< 0 : decays “off”, ≥ 0 : decays “on”) (default: 0);

fWeakDecay – flag to switch on/off weak hadron decays (<0 : decays “off”, ≥ 0 : decays “on”) (default: 0);

fEtaType – flag to specify longitudinal flow rapidity distribution (≤ 0 : uniform in the range $[-fYlmax, fYlmax]$, >0 : Gaussian with the dispersion $fYlmax$) (default: 1);

fTmuType – flag to use calculated chemical freeze-out temperature, baryon potential and strangeness potential as a function of **fSqrtS** (≤ 0 : specified by user values are taken, >0 : calculated according to the parameterization (23) values are used) (default: 0);

fCorrS – flag and value to include strangeness suppression factor γ_s with **fCorrS** value ($0 < fCorrS \leq 1$, if **fCorrS** ≤ 0 then it is calculated using its phenomenological dependence $\gamma_s = 1 - 0.386 \exp(-1.23T^{ch}/\mu_B)$ from [84]) (default: 1.).

Parameters for treatment of hard multi-parton part of the event.

fNhse1 – flag to switch on/off jet and hydro-state production (0: jet production “off” and hydro “on”, 1: jet production “on” and jet quenching “off” and hydro “on”, 2: jet production “on” and jet quenching “on” and hydro “on”, 3: jet production “on” and jet quenching “off” and hydro “off”, 4: jet production “on” and jet quenching “on” and hydro “off”) (default: 2);

fIshad – flag to switch on/off impact parameter dependent nuclear shadowing for gluons and light sea quarks (u,d,s) (0: shadowing “off”, 1: shadowing “on” for **fAw**=207., 197., 110. or 40.) (default: 1);

fPtmin – minimal transverse momentum transfer p_T^{\min} of hard parton-parton scatterings in GeV/c (the PYTHIA parameter **ckin(3)**=**fPtmin**)

PYQUEN energy loss model parameters:

fT0 – initial temperature T_0 (in GeV) of QGP for central Pb+Pb collisions at mid-rapidity (initial temperature for other centralities and atomic numbers will be calculated automatically) (allowed range is $0.2 < fT0 < 2.$);

fTau0 – proper QGP formation time τ_0 in fm/c ($0.01 < fTau0 < 10$);

fNf – number of active quark flavours N_f in QGP (**fNf**=0, 1, 2 or 3);

fIengl – flag to fix type of in-medium partonic energy loss (0: radiative and collisional loss, 1: radiative loss only, 2: collisional loss only) (default: 0);

fIanglu – flag to fix type of angular distribution of in-medium emitted gluons (0: small-angular (13), 1: wide-angular, 2: collinear) (default: 0).

Note that if specified by user value of input parameter extends out of the allowed range, its default value is used in HYDJET++ run.

A number of important PYTHIA parameters also may be changed/specified in **RunInputHydjet** file (they are not shown in Figs. 2 and 3). The rest PYTHIA parameters can be changed (if it is necessary) using corresponding common blocks in the file **progs_fortran.f**.

```

Number of events to generate
2
C.m.s. energy per nucleon pair, fSqrtS [GeV]
200.
Atomic weight of nuclei, fAw
197.
Flag of type of centrality generation, fBfix (=0 is fixed by fBfix, >0 distributed [fBfmin, fBmax])
1
Minimum impact parameter in units of nuclear radius, fBmin
0.
Maximum impact parameter in units of nuclear radius, fBmax
0.5
Fixed impact parameter in units of nuclear radius, fBfix
0.
Parameter to set random number seed, fSeed (=0 the current time is used, >0 the value fSeed is used)
0
Temperature at chemical freeze-out, fT [GeV]
0.165
Chemical baryon potential per unit charge, fMuB [GeV]
0.0285
Chemical strangeness potential per unit charge, fMuS [GeV]
0.007
Chemical isospin potential per unit charge fMuI3, [GeV]
-0.001
Temperature at thermal freeze-out, fTthFO [GeV]
0.1
Chemical potential of pi+ at thermal freeze-out, fMu_th_pip [GeV]
0.053
Proper time proper at thermal freeze-out for central collisions, fTau [fm/c]
8.
Duration of emission at thermal freeze-out for central collisions, fSigmaTau [fm/c]
2.
Maximal transverse radius at thermal freeze-out for central collisions, fR [fm]
10.
Maximal longitudinal flow rapidity at thermal freeze-out, fYlmax
3.3
Maximal transverse flow rapidity at thermal freeze-out for central collisions, fUmax
1.1
Momentum azimuthal anizotropy parameter at thermal freeze-out, fDelta
0.1
Spatial azimuthal anisotropy parameter at thermal freeze-out, fEpsilon
0.05
Flag to specify fDelta and fEpsilon values, fIfDeltaEpsilon (<=0 user's ones, >0 calculated)
0.
Flag to switch on/off hadron decays, fDecay (<0 decays off, >=0 decays on)
0.
Flag to switch on/off weak hadron decays, fWeakDecay: (<0 decays off, >=0 decays on)
0.
Flag to choose rapidity distribution, fEtaType (=0 uniform, >0 Gaussian with the dispersion Ylmax)
1.
Flag to use calculated T_ch, mu_B and mu_S as a function of fSqrtS, fTMuType
(<=0 user's ones, >0 calculated)
0
Flag and value to include the strangeness supression factor gamma_s with fCorrS value
(0<fCorrS <=1, if fCorrS <= 0. - it will be calculated)
1.
Flag to include jet (J)/jet quenching (JQ) and hydro (H) state production, fNhsel
2
Flag to switch on/off nuclear shadowing, fIshad (0 shadowing off, 1 shadowing on)
1
Minimal pt of parton-parton scattering in PYTHIA event, fPtmin [GeV/c]
3.4
Initial QGP temperature for central Pb+Pb collisions in mid-rapidity, fT0 [GeV]
0.3
Proper QGP formation time in fm/c, fTau0 (0.01<fTau0<10)
0.4
Number of active quark flavours in QGP, fNf (0, 1, 2 or 3)
2
Flag to fixe type of partonic energy loss, flengl
(0 radiative and collisional loss, 1 radiative loss only, 2 collisional loss only)
0
Flag to fix type of angular distribution of in-medium emitted gluons, flanglu
(0 small-angular, 1 wide-angular, 2 collinear).
0

```

Fig. 2. The input parameter file **RunInputHydjetRHIC200** (default).

```

Number of events to generate
2
C.m.s. energy per nucleon pair, fSqrtS [GeV]
5500.
Atomic weigth of nuclei, fAw
207.
Flag of type of centrality generation, fBfix (=0 is fixed by fBfix, >0 distributed [fBfmin, fBmax])
1
Minimum impact parameter in units of nuclear radius, fBmin
0.
Maximum impact parameter in units of nuclear radius, fBmax
0.5
Fixed impact parameter in units of nuclear radius, fBfix
0.
Parameter to set random number seed, fSeed (=0 the current time is used, >0 the value fSeed is used)
0
Temperature at chemical freeze-out, fT [GeV]
0.170
Chemical baryon potential per unit charge, fMuB [GeV]
0.
Chemical strangeness potential per unit charge, fMuS [GeV]
0.
Chemical isospin potential per unit charge fMuI3, [GeV]
0.
Temperature at thermal freeze-out, fTthFO [GeV]
0.13
Chemical potential of pi+ at thermal freeze-out, fMu_th_pip [GeV]
0.
Proper time proper at thermal freeze-out for central collisions, fTau [fm/c]
10.
Duration of emission at thermal freeze-out for central collisions, fSigmaTau [fm/c]
3.
Maximal transverse radius at thermal freeze-out for central collisions, fR [fm]
11.
Maximal longitudinal flow rapidity at thermal freeze-out, fYlmax
4.
Maximal transverse flow rapidity at thermal freeze-out for central collisions, fUmax
1.1
Momentum azimuthal anizotropy parameter at thermal freeze-out, fDelta
0.1
Spatial azimuthal anisotropy parameter at thermal freeze-out, fEpsilon
0.05
Flag to specify fDelta and fEpsilon values, fIfDeltaEpsilon (<=0 user's ones, >0 calculated)
0.
Flag to switch on/off hadron decays, fDecay (<0 decays off, >=0 decays on)
0.
Flag to switch on/off weak hadron decays, fWeakDecay: (<0 decays off, >=0 decays on)
0.
Flag to choose rapidity distribution, fEtaType (<= 0 uniform, >0 Gaussian with the dispersion Ylmax)
1.
Flag to use calculated T_ch, mu_B and mu_S as a function of fSqrtS, fTMuType
(<=0 user's ones, >0 calculated)
0
Flag and value to include the strangeness supression factor gamma_s with fCorrS value
(0<fCorrS <=1, if fCorrS <= 0., then it will be calculated)
1.
Flag to include jet (J)/jet quenching (JQ) and hydro (H) state production, fNhsel
2
Flag to switch on/off nuclear shadowing, fIshad (0 shadowing off, 1 shadowing on)
1
Minimal pt of parton-parton scattering in PYTHIA event, fPtmin [GeV/c]
7.
Initial QGP temperature for central Pb+Pb collisions in mid-rapidity, fT0 [GeV]
0.8
Proper QGP formation time in fm/c, fTau0 (0.01<fTau0<10)
0.1
Number of active quark flavours in QGP, fNf (0, 1, 2 or 3)
0
Flag to fixe type of partonic energy loss, flengl
(0 radiative and collisional loss, 1 radiative loss only, 2 collisional loss only)
0
Flag to fix type of angular distribution of in-medium emitted gluons, flanglu
(0 small-angular, 1 wide-angular, 2 collinear).
0

```

Fig. 3. The input parameter file **RunInputHydjetLHC5500** (default).

4.3 Output parameters and files

The program output is directed to a ROOT file specified by the user in the command line or by default to `RunOutput.root`. The output file contains a tree named `td`, which keeps the entire event record including primary particles and decay products with their coordinates and momenta information. Each decay product contains the unique index of its parent particle so that the entire event history may be obtained. Beside particle information, the output file contains also the following global output parameters for each event.

Bgen – generated value of impact parameter b in units of nucleus radius R_A ;
Sigin – total inelastic NN cross section at given energy **fSqrtS** (in mb);
Sigjet – hard scattering NN cross section at given **fSqrtS**, **fPtmin** (in mb);
Ntot – generated value of total event multiplicity ($N_{\text{tot}}=N_{\text{hyd}}+N_{\text{pyt}}$);
Nhyd – generated multiplicity of “soft” hydro-induced particles;
Npyt – generated multiplicity of “hard” jet-induced particles;
Njet – generated number N_{AA}^{jet} of hard parton scatterings with $p_T > \text{fPtmin}$;
Nbcol – mean number of binary NN sub-collisions $\overline{N}_{\text{bin}}$ (38) at given **Bgen**;
Npart – mean number of nucleons-participants $\overline{N}_{\text{part}}$ (39) at given **Bgen**.

The event output tree (`ROOT::TTree`) is organized as follows:

```
td->Branch("nev",&nev,"nev/I");
    // event number
td->Branch("Bgen",&Bgen,"Bgen/F");
    // generated impact parameter
td->Branch("Sigin",&Sigin,"Sigin/F");
    // total inelastic NN cross section
td->Branch("Sigjet",&Sigjet,"Sigjet/F");
    // hard scattering NN cross section
td->Branch("Ntot",&Ntot,"Ntot/I");
    // total event multiplicity
td->Branch("Nhyd",&Nhyd,"Nhyd/I");
    // multiplicity of hydro-induced particles
td->Branch("Npyt",&Npyt,"Npyt/I");
    // multiplicity of jet-induced particles
td->Branch("Njet",&Njet,"Njet/I");
    // number of hard parton-parton scatterings
td->Branch("Nbcol",&Nbcol,"Nbcol/I");
    // mean number of NN sub-collisions
td->Branch("Npart",&Npart,"Npart/I");
    // mean number of nucleon-participants
td->Branch("Px",&Px[0],"Px[npart]/F");
    // x-component of the momentum, in GeV/c
```

```

td->Branch("Py",&Py[0],"Py[npart]/F");
    // y-component of the momentum, in GeV/c
td->Branch("Pz",&Pz[0],"Pz[npart]/F");
    // z-component of the momentum, in GeV/c
td->Branch("E",&E[0],"E[npart]/F");
    // energy, in GeV
td->Branch("X",&X[0],"X[npart]/F");
    // x-coordinate at emission point, in fm
td->Branch("Y",&Y[0],"Y[npart]/F");
    // y-coordinate at emission point, in fm
td->Branch("Z",&Z[0],"Z[npart]/F");
    // z-coordinate at emission point, in fm
td->Branch("T",&T[0],"T[npart]/F");
    // proper time of particle emission, in fm/c
td->Branch("pdg",&pdg[0],"pdg[npart]/I");
    // Geant particle code
td->Branch("Mpdg",&Mpdg[0],"Mpdg[npart]/I");
    // Geant mother code (-1 for primordial)
td->Branch("type",&type[0],"type[npart]/I");
    // particle origin (=0: hydro, >0: jet)
td->Branch("Index",&Index[0],"Index[Ntot]/I");
    // unique zero based index of the particle
td->Branch("MotherIndex",&MotherIndex[0],"MotherIndex[Ntot]/I");
    // index of the mother particle (-1 if its a primary particle)
td->Branch("NDaughters",&NDaughters[0],"NDaughters[Ntot]/I");
    // number of daughter particles
td->Branch("Daughter1Index",&Daughter1Index[0],"Daughter1Index[Ntot]/I");
    // index of the first daughter (-1 if it does not exist)
td->Branch("Daughter2Index",&Daughter2Index[0],"Daughter2Index[Ntot]/I");
    // index of the second daughter
td->Branch("Daughter3Index",&Daughter3Index[0],"Daughter3Index[Ntot]/I");
    // index of the third daughter

```

The possibility to create event output written directly to histograms (in according to user's specification in the file `RunHadronSourceHisto.cxx`) is envisaged. The histogram output is directed by default to the file `RunOutputHisto.root` or to a file specified explicitly by the user in the command line.

4.4 Organization of the Fortran package

The hard, multi-jet part of HYDJET++ event is identical to the hard part of Fortran-written HYDJET [12,13] (version 1.5). The three Fortran files are placed in the directory PYQUEN.

pythia-6.4.11.f – PYTHIA event generator to simulate hard NN sub-collisions [15] (is used if **fNhse1**=1, 2, 3 or 4).

pyquen1_5.f – PYQUEN event generator to modify PYTHIA-produced hard events according to the corresponding partonic energy loss model [12,14] (is used if **fNhse1**=2 or 4), and to generate the spatial vertex of a jet production.

progs_fortran.f – main Fortran routine, which contains the following main subroutines and functions (the auxiliary subroutines and functions are not listed here).

- **subroutine_hyinit(fSqrtS,fAw,fIfb,fBmin,fBmax,fBfix)** – initializes PYTHIA, calculates cross sections **Sigin** and **Sigjet**, tabulates $T_A(b)$, $T_{AA}(b)$.

- **subroutine_hyevnt** – in each event generates the impact parameter value **Bgen** (if **fIfb** \neq 0), calculates numbers **Nbcol** and **Npart**, generates number of “successful” hard NN sub-collisions **Njet**, and calls **hyhard** subroutine.

- **subroutine_hyhard** – generates multi-parton production in **Njet** hard NN sub-collisions (with jet quenching if **fNhse1**=2 or 4, and with nuclear shadowing if **fIshad**=1), performs hadronization, and writes the final event output in the array **hyjets**.

- **subroutine_ggshad(inucl,x,q2,b,res,taf)** – adapts the parameterization of ratio of nuclear to nucleon parton distribution function **res** (**res**(1) for gluons and **res**(2) for sea quarks) in a given nucleus **inucl**, Bjorken **x** in the parton distribution, square of transverse momentum transfer in the hard scattering **q2**, and transverse position of jet production vertex relative to the nucleus center **b** (**taf** is the parametrized nuclear thickness function).

- **function_shad1(kfh,xbj,q2,r)** – in each event calculates the ratio of nuclear to nucleon parton distribution function (normalized by the atomic number) for the given parton code **kfh**, Bjorken **x** in a parton distribution **xbj**, square of transverse momentum transfer in the hard scattering **q2**, and transverse position of jet production vertex relative to the the nucleus center **r** (**call_ggshad** is performed).

4.5 Organization of the C++ package

The organization of the C++ package in HYDJET++ is similar to the FAST MC framework presented in [17,18]. The C++ source files are placed in the main directory.

The main modules of the C++ package.

- `RunHadronSource.cxx`, `RunHadronSourceHisto.cxx` – contains the `main` program. It handles the `InitialStateHydjet` class instance by calling the `ReadParams()`, `MultiIni()`, `Initialize()` and `Evolve()` member functions. The main program also creates the output ROOT tree and fills it with event information.
- `InitialState.cxx`, `InitialState.h` – contains virtual class `InitialState`. The `InitialState` class is responsible for initialization of the PDG particle database (`DatabasePDG`). The function `Evolve()` organizes the particle decays and updates the coordinate-time information on the particle list.
- `InitialStateHydjet.cxx`, `InitialStateHydjet.h` – contains the definition of the class `InitialStateHydjet`. This class inherits the upper class `InitialState`. The member function `ReadParams()` reads the parameters from the input file once per run. The function `MultiIni()` calculates the total particle specie multiplicities once per run. The `Initialize()` function generates the particles in the initial fireball. The `Evolve()` function, the heritage of the class `InitialState`, performs the decay of unstable particles.
- `HadronDecayer.cxx`, `HadronDecayer.h` – contains two functions called by the function `InitialState::Evolve()` to decay the resonances: `Decay()` and `GetDecayTime()`.

The service modules of the C++ package.

- `Particle.cxx`, `Particle.h` – contains the `Particle` class which handles all the track information (PDG properties, momenta, coordinate, indexes of parent particles and decay products).
- `ParticlePDG.cxx`, `ParticlePDG.h` – contains the definition of the class `ParticlePDG` which stores all the PDG properties of a particle specie. This class is used by the `Particle` class and by the `DatabasePDG` to organize the information.
- `DatabasePDG.cxx`, `DatabasePDG.h` – contains the definition of the class `DatabasePDG`. This class reads and handles all the particle specie definitions found in `particles.data` and all the decay channels found in `tabledecay.txt`.
- `DecayChannel.cxx`, `DecayChannel.h` – contains the `DecayChannel` class definition. This class stores the information for a single decay channel. A `ParticlePDG` instance uses `DecayChannel` objects to store informations regarding decay channels.
- `GrandCanonical.cxx`, `GrandCanonical.h` – contains the method to calculate the densities of energy, baryon and electric charge and particle numbers, within the grand canonical approach by means of the temperature and chem-

ical potentials.

- **StrangeDensity.cxx**, **StrangeDensity.h** – contains the method to calculate the strangeness density within the grand canonical description.
- **HankelFunction.cxx**, **HankelFunction.h** – computes modified Hankel function of zero, first and second orders.
- **StrangePotential.cxx**, **StrangePotential.h** – contains the method to calculate strange potential (if `fTMuTypeL=1`) from the initial strange density at given temperature and baryon potential.
- **EquationSolver.cxx**, **EquationSolver.h** – is used by **StrangePotential** class to calculate strangeness potential.
- **RandArrayFunction.cxx**, **RandArrayFunction.h** – defines several methods for shooting generally distributed random values, given a user-defined probability distribution function.
- **UKUtility.cxx**, **UKUtility.h** – contains the method **IsotropicR3** to generate the three-vector uniformly distributed on spherical surface, and the method **MomAntiMom** to calculate kinematical variables for two-body decays.
- **MathUtil.h** – contains some useful constant determinations.
- **HYJET_COMMONS.h** – contains the list of Fortran common blocks used by C++ package.

5 Installation instructions

HYDJET++ package is available via Internet. It can be downloaded from the corresponding web-page [85] as the archive **HYDJET++.ZIP**, which contains the following files and directories:

- the Makefile;
- the input files (**RunInputHydjet**, **RunInputHydjetRHIC200**, **RunInputHydjetLHC5500**);
- **HYDJET** directory with **inc** (*.h files), **src** (*.cxx files) and **SHARE** data files (**particle.data**, **tabledecay.txt**);
- **PYQUEN** directory with *.f files;
- **DOC** directory (with short description and update notes for new versions);
- **RootMacros** directory (the examples allowing one to obtain some physical results with HYDJET++, detailed comments are in the macros).

In order to run HYDJET++ on Linux one needs:

- 1) C++ and Fortran compilers;
- 2) ROOT libraries and include files.

The main program is in the files `RunHadronSource.cxx` (for ROOT tree output) or `RunHadronSourceHisto.cxx` (for ROOT histogram output). To compile the package one needs to use the following commands in the main HYDJET directory:

`make` (for ROOT tree output), or
`make -f Makefile_HISTO` (for ROOT histogram output).

Then the executable file `HYDJET` (or `HYDJET_HISTO`) is created in the same directory. Once the program is compiled, one can use the executables above to start a simulation run. The input file necessary to run `HYDJET++` must always be named `RunInputHydjet`, so after preparing this file according to the examples included in the package one can start the simulation with the command line: `./HYDJET` (or `./HYDJET_HISTO`). If an output file is not specified then the event records will be automatically directed to the file `RunOutput.root` (or `RunOutputHisto.root`).

6 Validation of HYDJET++ with experimental RHIC data

It was demonstrated in previous papers that FAST MC model can describe well the bulk properties of hadronic state created in Au+Au collisions at RHIC at $\sqrt{s} = 200A$ GeV (such as particle number ratios, low- p_T spectra, elliptic flow coefficients $v_2(p_T, b)$, femtoscopic correlations in central collisions) [17,18], while HYDJET model is capable of reproducing the main features of jet quenching pattern at RHIC (high- p_T hadron spectra and the suppression of azimuthal back-to-back correlations) [12]. Since soft and hard hadronic states in HYDJET++ are simulated independently, a good description of hadroproduction at RHIC in a wide kinematic range can be achieved, moreover a number of improvements in FAST MC and HYDJET have been done as compared to earlier versions. A number of input parameters of the model can be fixed from fitting the RHIC data to various physical observables (listed in Fig. 2).

- (1) **Ratio of hadron abundances.** It is well known that the particle abundances in heavy ion collisions in a wide energy range can be reasonable well described within statistical models based on the assumption that the produced hadronic matter reaches thermal and chemical equilibrium. The thermodynamical parameters $\tilde{\mu}_B = 0.0285$ GeV, $\tilde{\mu}_S = 0.007$ GeV, $\tilde{\mu}_Q = -0.001$, the strangeness suppression factor $\gamma_s = 1$, and the chemical freeze-out temperature $T^{\text{ch}} = 0.165$ GeV have been fixed in [17] from fitting the RHIC data to various particle ratios near mid-rapidity in central Au+Au collisions at $\sqrt{s} = 200A$ GeV (π^-/π^+ , \bar{p}/π^- , K^-/K^+ , K^-/π^- , \bar{p}/p , $\bar{\Lambda}/\Lambda$, $\bar{\Xi}/\Xi$, ϕ/K^- , Λ/p , Ξ^-/π^-).

- (2) **Low- p_T hadron spectra.** Transverse momentum p_T and transverse mass m_T hadron spectra (π^+ , K^+ and p with $m_T < 0.7$ GeV/ c^2) near mid-rapidity at different centralities of Au+Au collisions at $\sqrt{s} = 200A$ GeV were analyzed in [18]. The slopes of these spectra allow the thermal freeze-out temperature $T^{\text{th}} = 0.1$ GeV and the maximal transverse flow rapidity in central collisions $\rho_u^{\text{max}}(b = 0) = 1.1$ to be fixed.
- (3) **Femtoscopic correlations.** Because of the effects of quantum statistics and final state interactions, the momentum (HBT) correlation functions of two or more particles at small relative momenta in their c.m.s. are sensitive to the space-time characteristics of the production process on the level of fm . The space-time parameters of thermal freeze-out region in central Au+Au collisions at $\sqrt{s} = 200A$ GeV have been fixed in [18] by means of fitting the three-dimensional correlation functions measured for $\pi^+\pi^+$ pairs and extracting the correlation radii R_{side} , R_{out} and R_{long} : $\tau_f(b = 0) = 8$ fm/ c , $\Delta\tau_f(b = 0) = 2$ fm/ c , $R_f(b = 0) = 10$ fm.
- (4) **Pseudorapidity hadron spectra.** The PHOBOS data on η -spectra of charged hadrons [86] at different centralities of Au+Au collisions at $\sqrt{s} = 200A$ GeV have been analyzed to fix the particle densities in the mid-rapidity region and the maximum longitudinal flow rapidity $\eta_{\text{max}} = 3.3$ (Fig. 4). Since mean “soft” and “hard” hadron multiplicities depend on the centrality in different ways (they are roughly proportional to $\overline{N_{\text{part}}(b)}$ and $\overline{N_{\text{bin}}(b)}$ respectively), the relative contribution of soft and hard parts to the total event multiplicity can be fixed through the centrality dependence of $dN/d\eta$. The corresponding contributions from hydro- and jet-parts are determined by the input parameters $\mu_{\pi}^{\text{eff th}} = 0.053$ GeV and $p_T^{\text{min}} = 3.4$ GeV/ c respectively.
- (5) **High- p_T hadron spectra.** High transverse momentum hadron spectra ($p_T \gtrsim 2 - 4$ GeV/ c) are sensitive to parton production and jet quenching effects. Thus fitting the measured high- p_T tail allows the extraction of PYQUEN energy loss model parameters. We assume the QGP formation time $\tau_0 = 0.4$ fm/ c and the number of active quark flavours $N_f = 2$. Then the reasonable fit of STAR data on high- p_T spectra of charged pions at different centralities of Au+Au collisions at $\sqrt{s} = 200A$ GeV [87] is obtained with the initial QGP temperature $T_0 = 0.3$ GeV (Fig. 5).
- (6) **Elliptic flow.** The elliptic flow coefficient v_2 (which is determined as the second-order Fourier coefficient in the hadron distribution over the azimuthal angle φ relative to the reaction plane angle ψ_R , so that $v_2 \equiv \langle \cos 2(\varphi - \psi_R) \rangle$) is an important signature of the physics dynamics at early stages of non-central heavy ion collisions. According to the typical hydrodynamic scenario, the values $v_2(p_T)$ at low- p_T ($\lesssim 2$ GeV/ c) are determined mainly by the internal pressure gradients of an expanding fireball during the initial high density phase of the reaction (and it is sensitive to the momentum and azimuthal anisotropy parameters δ and ϵ in the frameworks of HYDJET++), while elliptic flow at high- p_T is generated in HYDJET++ (as well as in other jet quenching models) due to

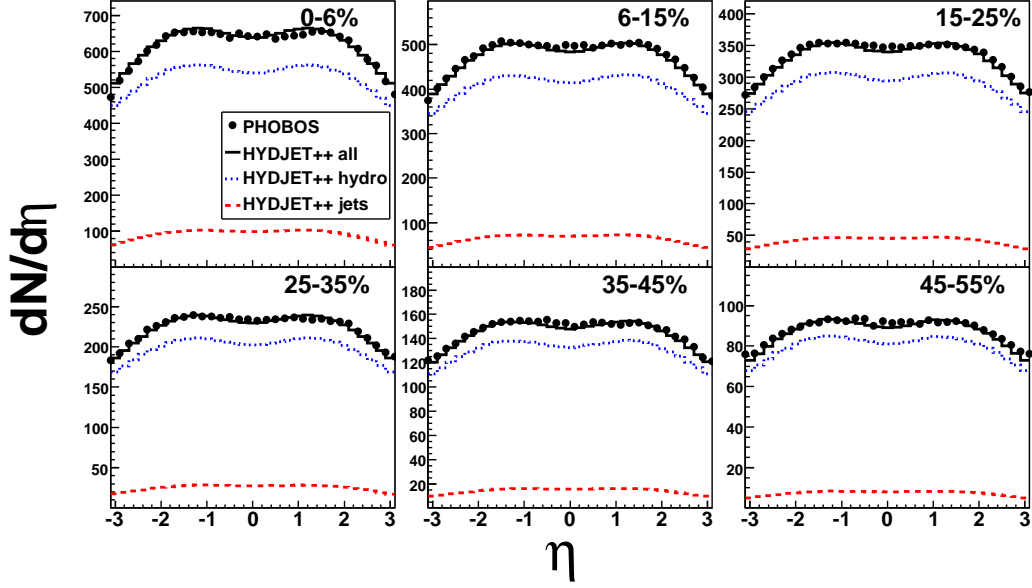


Fig. 4. The pseudorapidity distribution of charged hadrons in Au+Au collisions at $\sqrt{s} = 200A$ GeV for six centrality sets. The points are PHOBOS data [86], histograms are the HYDJET++ calculations (solid – total, dotted – jet part, dashed – hydro part).

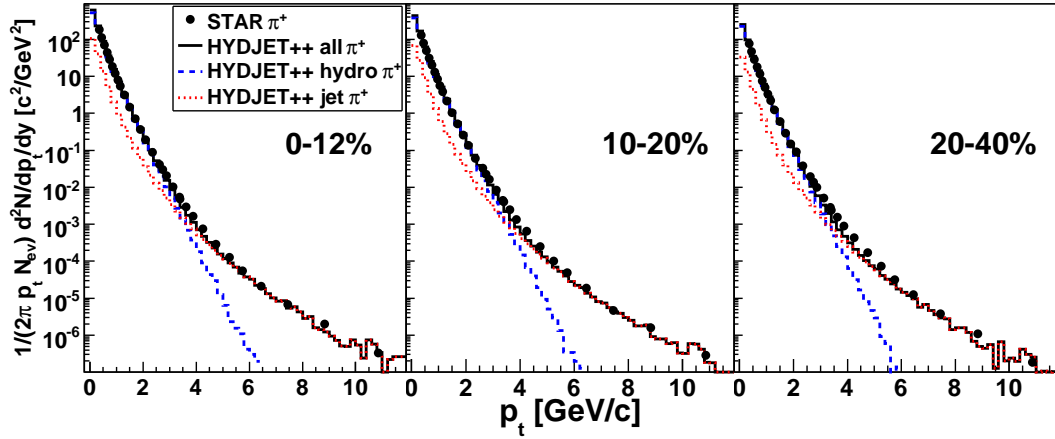


Fig. 5. The transverse momentum distribution of positively charged pions in Au+Au collisions at $\sqrt{s} = 200A$ GeV for three centrality sets. The points are STAR data [87], histograms are the HYDJET++ calculations (solid – total, dotted – jet part, dashed – hydro part).

the partonic energy loss in an azimuthally asymmetric volume of QGP. Figure 6 shows the measured by the STAR Collaboration transverse momentum dependence of the elliptic flow coefficient v_2 of charged hadrons in Au+Au collisions at $\sqrt{s} = 200A$ GeV for two centrality sets [88]. The values of δ and ϵ estimated for each centrality are written on the plots. Note that the choice of these parameters does not affect any azimuthally integrated physics observables (such as hadron multiplicities, η - and p_T -spectra, etc.), but only their differential azimuthal dependences.

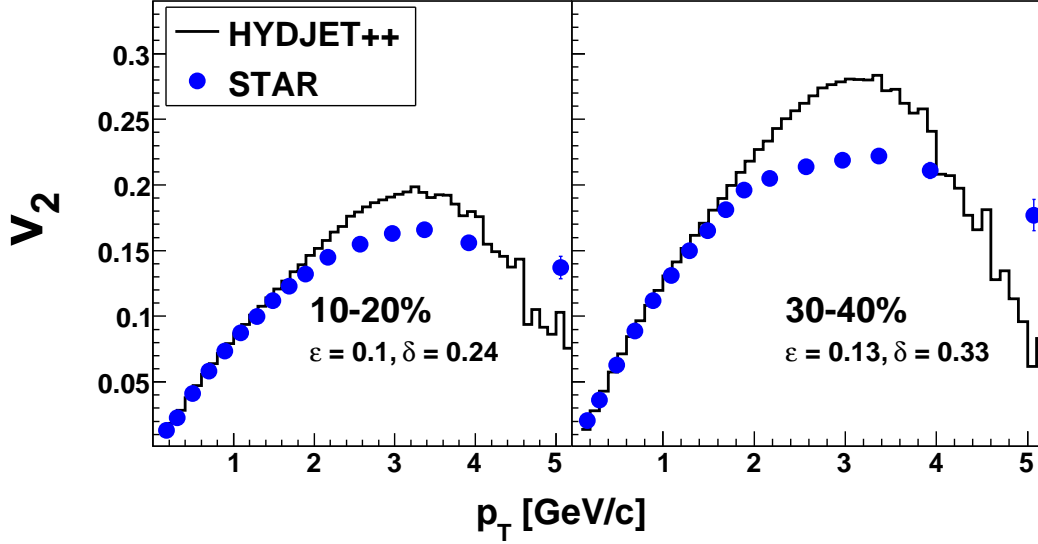


Fig. 6. The transverse momentum dependence of the elliptic flow coefficient v_2 of charged hadrons in Au+Au collisions at $\sqrt{s} = 200A$ GeV for two centrality sets. The points are STAR data [88], histograms are the HYDJET++ calculations.

7 Test run description

The set of macros for comparison of various physics observables with the experimental data obtained for different centralities of Au+Au collisions at $\sqrt{s} = 200A$ GeV are in the directory `RootMacros`.

- `fig_eta_Phobos.C`, `fig_eta_Phobos_read.C` – the charged hadron pseudo-rapidity spectra are generated (Fig. 4). To start the generation, the user should type: `root -l fig_eta_Phobos.C`, or `root -l fig_eta_Phobos_read.C`. In the latter case, the number of events should be specified in the macro `fig_eta_Phobos_read.C`. The PHOBOS data [86] are in the directory `eta_PHOBOS`.

- `fig_PTH_STAR.C`, `fig_PTH_STAR_read.C` – the positive pion p_T -spectra are generated (Fig. 5). To start the generation, the user should type: `root -l fig_PTH_STAR.C`, or `root -l fig_PTH_STAR_read.C`. In the latter case, the number of events should be specified in the macro `fig_PTH_STAR_read.C`. The STAR data [87] are in the directory `HPT_STAR`.

- `fig_v2_STAR.C`, `fig_v2_STAR_read.C` – the elliptic flow coefficients $v_2(p_T)$ of charged hadrons are generated (Fig. 6). To start the generation, the user should type: `root -l fig_v2_STAR.C`, or `root -l fig_v2_STAR_read.C`. In the latter case, the number of events should be specified in the macro `fig_v2_test_read.C`. The STAR data [88] are in the directory `v2_STAR`.

8 Conclusion

Ongoing and future experimental studies of relativistic heavy ion collisions require the development of new Monte-Carlo event generators and improvement of existing ones. The main advantage of MC technique for the simulation of multiple hadroproduction is that it allows visual comparison of theory and data, including if necessary the detailed detector acceptances, responses and resolutions. The realistic MC event generator should include a maximum possible number of observable physical effects which are important to determine the event topology: from bulk properties of soft hadroproduction (domain of low transverse momenta p_T) to hard multi-parton production in hot QCD-matter, which reveals itself in spectra of high- p_T particles and hadronic jets.

The HYDJET++ event generator has been developed to simulate relativistic heavy ion AA collisions considered as a superposition of the soft, hydro-type state and the hard state resulting from multi-parton fragmentation. It includes detailed treatment of soft hadroproduction (collective flow phenomena and resonance decays) as well as hard parton production, and takes into account the known medium effects (as jet quenching and nuclear shadowing). The main program is written in the object-oriented C++ language under the ROOT environment. The hard part of HYDJET++ is identical to the hard part of Fortran-written HYDJET generator and it is included in the generator structure as a separate directory. The soft part of HYDJET++ event is the “thermal” hadronic state generated on the chemical and thermal freeze-out hypersurfaces obtained from the parameterization of relativistic hydrodynamics with preset freeze-out conditions (the adapted C+ code FAST MC). HYDJET++ is capable of simultaneous reproducing the various hadronic observables measured in heavy ion collisions at RHIC for different centrality sets in a wide kinematic range: ratio of hadron yields, pseudorapidity and transverse momentum spectra (for both low- and high- p_T domains), elliptic flow coefficients $v_2(p_T)$, femtoscopic correlations. Although the HYDJET++ generator is optimized for RHIC and LHC energies, in practice it can be also used for studying of multi-particle production in a wider energy range down to $\sqrt{s} \sim 10$ GeV per nucleon pair at other heavy ion experimental facilities.

9 Acknowledgements

Discussions with L.V. Bravina, D. d’Enterria, G.H. Eyyubova, A.I. Demin, I.M. Dremin, A.B. Kaidalov, Iu.A. Karpenko, O.L. Kodolova, V.L. Korotkikh, R. Lednicky, C. Loizides, C. Mironov, S.V. Molodtsov, A. Morsch, T.A. Pocheptsov, C. Roland, L.I. Sarycheva, Yu.M. Sinyukov, T. Sjostrand, C.Yu. Teplov, I.N. Vardanyan, G. Veres, I. Vitev, B. Wyslouch, Y. Yilmaz,

E.E. Zabrodin, B.G. Zakharov and G.M. Zinovjev are gratefully acknowledged. This work was supported by Russian Foundation for Basic Research (grants No 08-02-91001 and No 08-02-92496), Grants of President of Russian Federation (No 107.2008.2 and 1456.2008.2) and Grant of INTAS No 05-103-7484.

References

- [1] R. Brun and F. Rademakers, Nucl. Instrum. Meth. A **389** (1997) 81; (<http://root.cern.ch>).
- [2] Proceedings of 18th International Conference on Ultra-Relativistic Nucleus-Nucleus Collisions “Quark Matter 2005” (Budapest, Hungary, August, 4-9, 2005), Nucl. Phys. A **774** (2006).
- [3] Proceedings of 19th International Conference on Ultra-Relativistic Nucleus-Nucleus Collisions “Quark Matter 2006” (Shanghai, China, November 14-20, 2006), J. Phys. G **34** S (2007).
- [4] Proceedings of 20th International Conference on Ultra-Relativistic Nucleus-Nucleus Collisions “Quark Matter 2008” (Jaipur, India, February 4-10, 2008), J. Phys. G, in press.
- [5] F. Carminati *et al.* [ALICE Collaboration], J. Phys. G **30** (2004) 1517.
- [6] B. Alessandro *et al.* [ALICE Collaboration], J. Phys. G **32** (2006) 1295.
- [7] D. d’Enterria *et al.* [CMS Collaboration], J. Phys. G **34** (2007) 2307.
- [8] N. Armesto (ed.) *et al.*, J. Phys. G **35** (2008) 054001.
- [9] A. Accardi *et al.*, CERN-2004-009-B, e-print: [hep-ph/0310274](http://arxiv.org/abs/hep-ph/0310274).
- [10] M. Bedjidian *et al.*, CERN-2004-009-C, e-print: [hep-ph/0311048](http://arxiv.org/abs/hep-ph/0311048).
- [11] F. Arleo *et al.*, CERN-2004-009-C, e-print: [hep-ph/0311131](http://arxiv.org/abs/hep-ph/0311131).
- [12] I.P. Lokhtin and A.M. Snigirev, Eur. Phys. J. C **45** (2006) 211.
- [13] <http://cern.ch/lokhtin/hydro/hydjet.html> .
- [14] <http://cern.ch/lokhtin/pyquen> .
- [15] T. Sjostrand, S. Mrenna and P. Skands, JHEP **0605** (2006) 026 (<http://home.thep.lu.se/~torbjorn/Pythia.html>).
- [16] K. Tywoniuk, I.C. Arsene, L. Bravina, A.B. Kaidalov and E. Zabrodin, Phys. Lett. B **657** (2007) 170.
- [17] N.S. Amelin *et al.*, Phys. Rev. C **74** (2006) 064901.
- [18] N.S. Amelin *et al.*, Phys. Rev. C **77** (2008) 014903.

- [19] G. Torrieri *et al.*, Comput. Phys. Commun. **167** (2005) 229.
- [20] R.C. Hwa (ed.) and X.N. Wang (ed.), “Quark-gluon plasma”, River Edge, USA: World Scientific (2004).
- [21] D. d’Enterria, J. Phys. **G 34** (2007) S53.
- [22] P. Braun-Munzinger and J. Stachel, Nature **448** (2007) 302.
- [23] I. Arsene *et al.* [BRAHMS Collaboration], Nucl. Phys. **A 757** (2005) 1.
- [24] B.B. Back *et al.* [PHOBOS Collaboration], Nucl. Phys. **A 757** (2005) 28.
- [25] J. Adams *et al.* [STAR Collaboration], Nucl. Phys. **A 757** (2005) 102.
- [26] K. Adcox *et al.* [PHENIX Collaboration], Nucl. Phys. **A 757** (2005) 184.
- [27] R. Baier, D. Schiff and B.G. Zakharov, Annual Rev. Nucl. Part. Sci. **50** (2000) 37.
- [28] X.-N. Wang, Phys. Lett. **B 579** (2004) 299.
- [29] U. Heinz, J. Phys. **G 31** (2005) S717.
- [30] P. Senger *et al.*, “The Compressed Baryonic Matter Experiment at the Future Accelerator Facility in Darmstadt: Letter of Intent”, GSI, Darmstadt, 2004.
- [31] A.N. Sissakian *et al.*, “The Multipurpose Detector (MPD) to study Heavy Ion Collisions at NICA: Letter of Intent”, JINR, Dubna, 2008.
- [32] M.A. Stephanov, K. Rajagopal and E.V. Shuryak, Phys. Rev. Lett. **81** (1998) 4816.
- [33] M. Gyulassy and X.-N. Wang, Comput. Phys. Commun. **83** (1994) 307.
- [34] K. Zapp, G. Ingelman, J. Rathsman, J. Stachel and U.A. Wiedemann, CERN-PH-TH-2008-067, e-print: arXiv:0804.3568 [hep-ph].
- [35] H. Pi, Comput. Phys. Commun. **71** (1992) 173.
- [36] A. Tai and B.-H. Sa, Comput. Phys. Commun. **116** (1999) 353.
- [37] A. Kisiel, T. Taluc, W. Broniowski, W. Florkowski, Comput. Phys. Commun. **174** (2006) 669.
- [38] S.A. Bass *et al.*, Prog. Part. Nucl. Phys. **41** (1998) 255.
- [39] N.S. Amelin and L.V Bravina, Sov. J. Nucl. Phys. **51** (1990) 133.
- [40] B. Zhang, C.M. Ko, B.A. Li, and Z.W. Lin, Phys. Rev. C **61** (2000) 067901.
- [41] B. Zhang, Comput. Phys. Commun. **109** (1998) 193.
- [42] T. Hirano and T. Nara, Nucl. Phys. **A 743** (2004) 305.
- [43] X.-N. Wang, M. Gyulassy and M. Plumer, Phys. Rev. **D 51** (1995) 3436.

- [44] R. Baier, Yu.L. Dokshitzer, A.H. Mueller, S. Peigne and D. Schiff, Nucl. Phys. **B 483** (1997) 291.
- [45] B.G. Zakharov, JETP Lett. **65** (1997) 615.
- [46] M. Gyulassy, P. Levai and I. Vitev. Phys. Rev. Lett. **85** (2000) 5535.
- [47] U.A. Wiedemann, Nucl. Phys. **A 690** (2001) 731.
- [48] L.D. Landau and I.Ya. Pomeranchuk, Dokl. Akad. Nauk SSSR **92** (1953) 535.
- [49] A.B. Migdal, Phys. Rev. **103** (1956) 429.
- [50] J.D. Bjorken, Fermilab publication Pub-82/29-THY (1982).
- [51] E. Braaten and M. Thoma, Phys. Rev. **D 44** (1991) 1298.
- [52] I.P. Lokhtin and A.M. Snigirev, Eur. Phys. J. **C 16** (2000) 527.
- [53] J. Randrup and S. Mrówczyński, Phys. Rev. **C 68** (2003) 034909.
- [54] Y.A. Markov, M.A. Markova and A.N. Vall, Annals Phys. **309** (2004) 93.
- [55] M.G. Mustafa and M.H. Thoma, Acta Phys. Hung. **A 22** (2005) 93.
- [56] S. Peigne, P.-B. Gossiaux and T. Gousset, JHEP **0604** (2006) 011.
- [57] K. Zapp, G. Ingelman, J. Rathsmann and J. Stachel, Phys. Lett. **B 637** (2006) 179.
- [58] A. Adil, M. Gyulassy, W.A. Horowitz and S. Wicks, Phys. Rev. **C 75** (2007) 044906.
- [59] M. Djordjevic, Phys. Rev. **C74** (2006) 064907.
- [60] J.-e Alam, A.K. Dutt-Mazumder and P. Roy, Nucl. Phys. **A 785** (2007) 245.
- [61] A. Ayala, J. Magnin, L.M. Montano and E. Rojas, Phys. Rev. **C 77** (2008) 044904.
- [62] X.-N. Wang, Phys. Lett. **B 650** (2007) 213.
- [63] R. Baier, Yu. L. Dokshitzer, A.H. Mueller and D. Schiff, Phys. Rev. **C 60** (1999) 064902.
- [64] R. Baier, Yu. L. Dokshitzer, A.H. Mueller and D. Schiff, Phys. Rev. **C 64** (2001) 057902.
- [65] X.-N. Wang and X.-F. Guo, Nucl. Phys. **A 696** (2001) 788.
- [66] I. Vitev, Phys. Lett. **B 630** (2005) 78.
- [67] E. Wang and X.-N. Wang, Phys. Rev. Lett. **87** (2001) 142301.
- [68] Yu.L. Dokshitzer and D. Kharzeev, Phys. Lett. **B 519** (2001) 199.
- [69] J.D. Bjorken, Phys. Rev. **D 27** (1983) 140.

- [70] C.W. deJager, H. deVries and C. deVries, Atomic Data and Nuclear Data Tables **14** (1974) 485.
- [71] I.P. Lokhtin and A.M. Snigirev, Phys. Lett. **B 440** (1998) 163.
- [72] V.N. Gribov, Sov. Phys. JETP **29** (1969) 483.
- [73] A. Aktas *et al.*, H1 Collaboration, Eur. Phys. J. C **48** (2006) 715; *ibid.* **48** (2006) 749.
- [74] J. Rafelski, Phys. Lett. **B 262** (1981) 333.
- [75] G.D. Yen, M.I. Gorenstein, W. Greiner and S.N. Yang, Phys. Rev. **C 56** (1997) 2210.
- [76] S.R. de Groot, W.A. van Leeuwen, Ch.G. van Weert, Relativistic kinetic theory. Principles and Applications, North-Holland Publishing Company, Amsterdam-New York-Oxford, 1980.
- [77] Yu.M. Sinyukov, S.V. Akkelin and A.Yu. Tolstykh, Nukleonika **43** (1998) 369.
- [78] J. Cleymans, H. Oeschler, K. Redlich and S. Wheaton, Phys. Rev. **C 73** (2006) 034905.
- [79] S.V. Akkelin, P. Braun-Munzinger and Yu.M. Sinyukov, Nucl. Phys. **A 710** (2002) 439.
- [80] J. Adams *et al.* [STAR Collaboration], Phys. Rev. Lett. **93** (2004) 012301.
- [81] S.S. Adler *et al.* [PHENIX Collaboration], Phys. Rev. Lett. **93** (2004) 152302.
- [82] U. Wiedemann, Phys. Rev. **C 57** (1998) 266.
- [83] R.J. Glauber and G. Matthiae, Nucl. Phys. **B 21** (1970) 135.
- [84] F. Becattini, J. Manninen and M. Gazdzicki, Phys. Rev. **C 73** (2006) 044905.
- [85] <http://cern.ch/lokhtin/hydjet++> .
- [86] B.B. Back *et al.* [PHOBOS Collaboration], Phys. Rev. Lett. **91** (2003) 052303.
- [87] B.I. Abelev *et al.* [STAR Collaboration], Phys. Rev. Lett. **97** (2006) 152301.
- [88] J. Adams *et al.* [STAR Collaboration], Phys. Rev. **C 72** (2005) 014904.